CLIMATE WARMING IMPACTS ON ALPINE SNOWPACKS IN WESTERN NORTH AMERICA

SUZAN L. LAPP

B.Sc., University of Lethbridge, 2000

A Thesis
Submitted to the School of Graduate Studies
of the University of Lethbridge
in Partial Fulfillment of the
Requirements for the Degree

Masters of Science

Department of Geography
University of Lethbridge
Lethbridge, Alberta, Canada

Abstract

A wide area assessment of forecast changes in wintertime synoptic conditions over western North America is combined with a meso-scale alpine hydrometeorology model to evaluate the joint impact(s) of forecast climate change on snowpack conditions in an alpine watershed in the southern Canadian Rockies. The synoptic analysis was used to generate long-term climate time series scenarios using the CCCma CGCM1. An alpine hydrometeorology model is used to predict changes in wintertime precipitation at the watershed scale. A mass balance snow model is utilized to predict the overall snow accumulation throughout a watershed. A vapour transfer model has been incorporated in the snow model to estimate snow volumes more accurately. The synoptic analysis and GCM output forecasts a modest increase in both winter precipitation and temperatures in the study area, resulting in a decline of winter snow accumulations, and hence an expected decline in spring runoff.

Acknowledgments

These past two years have been the most challenging yet rewarding years of my life. I definitely could not have done it without the support and encouragement of my committee members, Dr. James Byrne, Dr. Stefan Kienzle, Dr. Ivan Townshend and Dr. Larry Flanagan. I would like to thank Dr. Shawn Marshall (University of Calgary) for acting as my external examiner at my defense.

I owe an incredible thanks to Jim for allowing me this opportunity to pursue a goal that I had never once really considered or thought was possible. It has been an incredible privilege to work with you these past years. You are truly a mentor and friend. Although I admit, occasionally, I was full of complaints, I wouldn't change a thing.

A special thanks to Dennis Sheppard for helping me struggle through my computer illiterate days, helping me acquire the knowledge I have today. I must also thank Diedre Davidson, whom has become one of my best friends. Thanks for leading me astray. Truly some of the best memories I have are of Grad School.

My greatest thanks go to my family. My parents who always stood behind me and gave that little extra bit of encouragement I often needed, and my brother, Shane, who was always there to lend an ear and put a smile on my face. You have been the best family a girl could ask for.

This one's for you Dad.

Table of Contents

List of Tables

List of Figures

List of Abbreviations

$1xCO_2$	defined as the period of 1962-85 based of CGCM1 data
$2xCO_2$	defined as the period of period of 2021-50 based of CGCM1 data
ABL	Atmospheric boundary layer
CGCM1	Canadian Climate Centre first generation coupled General Circulation Model
CCCma	Canadian Climate Centre for Modeling and Analysis
GCM	Global circulation model
LAI	Leaf Area Index
SWE	Snow water equivalent

Chapter 1

Overview

1.1 Introduction

Snow accumulation over-winter in alpine regions provides most of the surface water supplies available for Western North America (Grant and Kahan, 1974). Global Circulation models forecast wintertime warming of close to four degrees Celsius (Saunders and Byrne, 1994) within fifty to one hundred years. Detailed analyses of changes to synoptic (precipitation) patterns over western North America forecast that precipitation in winter will change little on the plains (Saunders and Byrne, 1996), but in the alpine regions substantial potential exists for increased winter precipitation in the northern Rockies (Canada and the northwestern States) and a serious decline in winter precipitation in the southern Rocky Mountain States (Byrne et al. 1999). Little information is available on how increasing temperature will affect precipitation storage as snow as opposed to liquid (rain). Snow-runoff ratios are much higher than rainfall-runoff ratios. Therefore, if much of the winter precipitation falls as rain due to climate warming then the net results may be a decline in streamflow water supplies in many years despite an increase in winter precipitation total in northern regions.

This thesis investigates possible changes to winter snow accumulation and ablation (mass balance), and total spring snow pack for the upper Oldman watershed in western Canada. The work will build on and combine results from Sheppard (1996); Saunders and Byrne (1994; 1996); and Byrne et al. (1999) to model changes

to snow mass balance for alpine watersheds using a detailed alpine micrometeorology model SIMGRID (Sheppard, 1996) and output from the Canadian Centre for Climate Modeling and Analysis (CCCma) First Generation coupled general circulation model (CGCM1).

1.2 Global Warming

Although the Earth has experienced major climate changes throughout its history, there is evidence that the apparent trend towards warming in this past century is due to human activities (Pearman, 1992). Processes such as the combustion of fossil fuels contribute excess amounts of greenhouse gases to the atmosphere. This has led to predictions that atmospheric concentrations of carbon dioxide in particular will double. Mathematical models of climate processes suggest that a doubling of pre-industrial levels of CO_2 would cause the average temperature of the Earth's surface to rise between 1.5-4.5°C (IPCC 1996a, 1996b). At a smaller scale the prospect of a warmer Earth raises concerns with respect to changes in regional climate and associated water resources.

Present concerns about climate change arise from two basic and undisputed facts. The first is that greenhouse gases, such as carbon dioxide and nitrous oxides, retard the rate at which the earth loses heat to space and thus contribute to the warming of the lower atmosphere. The second is that concentrations of these gases are increasing as a result of human activities (Hengeveld, 2000). Figure 1.1 shows the overall annual increase in CO_2 between 1958 and 2000.

Not only are humans adding CO_2 to the environment, we are also destroying natural carbon sinks used to store CO_2 (Rama et al. 1999). Forests act as carbon sinks, removing carbon dioxide from the atmosphere (Williams, 1999).

To determine the likely effect of a change such as an increase in greenhouse gas concentrations on the climate system, it is necessary to look at how the system as a whole responds. To do this, climate models are essential, because they integrate the main processes that occur within the climate system and calculate the adjustments of its various elements as they respond to the original change.

1.3 Objectives

The overall objectives of this thesis are to forecast what the impact that future temperature and precipitation variations will have on spring snow water equivalent (SWE) for a representative watershed in the Western Canadian Rocky Mountains. The "future" scenario is based on an approximate doubling of CO_2 concentrations in the atmosphere, as forecast by the Canadian Climate Centre CGCM1. These changes are forecast to occur from 2020 to 2050.

To achieve the overall objective of the thesis, the following sub objectives or milestones were addressed.

- Develop future precipitation and temperature scenarios based on the CCCma CGCM1
- Modify an over-winter snowpack mass balance modeling routine to incorporate vapour transfer (sublimation and condensation) to and from the snowpack
- Develop historical and future snow cover maps for the study basin
- Carry out a comparative analysis of historical and future spring snow water equivalent conditions for the study watershed.

1.4 Thesis Format

This thesis is laid out in a paper style format as follows.

Chapter 1 – Introduction.

Chapter 2 - Literature review.

Chapter 3 – Paper under review by the *International Journal of Climatology.*

Chapter 4 – Paper accepted for presentation at the Western Snow Conference; and for review by *Hydrological Processes.*

Chapter 5 – Summary and Recommendations.

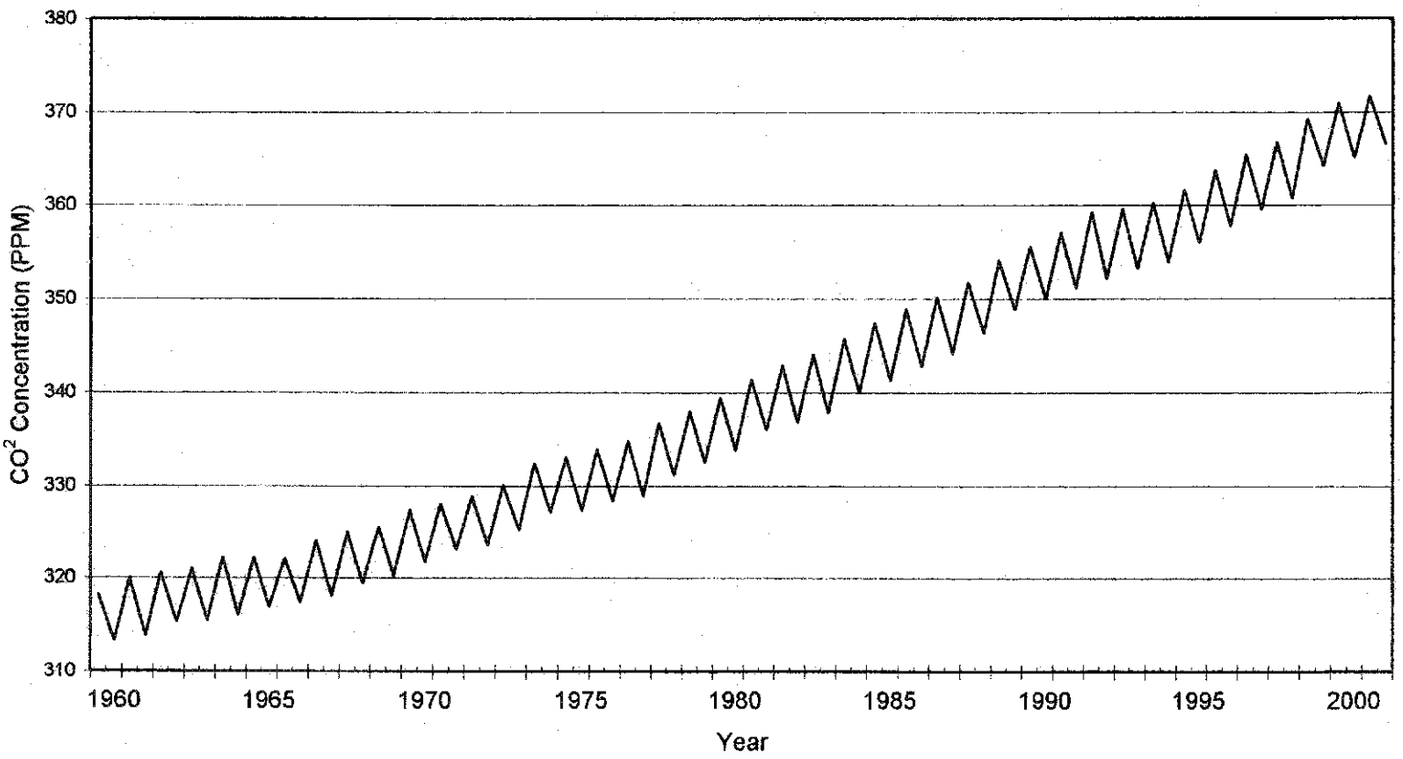

Figure 1.1 Upward trend in atmospheric carbon dioxide levels as measured at Mauna Loa Observatory, Hawaii, 1958-2000. (Keeling and Whorf, 2001).

Chapter 2
Literature Review

2.1 Introduction

The following literature review covers the concepts, ideas and methodologies that are used in this research to achieve each milestone.

2.2 General Circulation Models

Three dimensional mathematical computer-based global climate models, called General Circulation Models (GCMs), are used to simulate past as well as future global climate conditions. Some of the more common models discussed in the literature are those of: the Goddard Institute for Space Studies (GISS) (Rind et al. 2001 (a); Rind et al. 2001 (b); Shindell et al. 2001), the Geophysical Fluid Dynamics Laboratory (GFDL) (DeMaria and Tuleya, 2000; Hamilton et al. 2001), the Hadley Centre for Climate Prediction and Research (HADLEY) (Gordon et al. 2000; Jones et al. 1999; Venzke et al. 1999; Gregory et al. 2001) and the Canadian Climate Centre (CCC) (Flato et al. 2000; Fyfe and Flato, 1999; Boer et al. 2000). The output from such GCM's is currently used to predict regional impacts of climate change in many studies. Unfortunately, GCM's are typically based upon a widely spaced resolution covering large areas of the Earths surface making them less than ideal for simulating temperature and precipitation at a smaller scale (McFarlane et al. 1992; Hewitson and Crane, 1992).

The current generation of these models includes a realistic geography, interactive clouds, terrestrial vegetation and hydrology, polar sea ice, and, to a greater or lesser degree, some dynamic or thermodynamic interaction with the ocean surface. Despite differences in numerical methods, parameterization schemes, and grid-box resolution, past and current models do a reasonable job of simulating the large-scale feature of the

climate system (Schlesinger and Mitchell, 1987; Widemann and Bretherton, 1999; McFarlane et al. 1992). All of the recent GCM predictions show similar results when averaged annually and over a hemisphere. Where the models tend to show substantial disagreement, however, is in their regional-scale predictions of climate change. The few model intercomparison studies that have been undertaken (National Research Council 1983; Schlesinger and Mitchell, 1987; Grotch and MacCracken, 1991; Rinke et al. 2000;Valdes, 2000;) all indicate that models do a relatively poor job of simulating the atmosphere over less than the monthly averaged hemispheric time and space scales. Societies' ability to plan for environmental change will be dictated largely by the degree to which it can predict the regional impacts of future climates. A major problem thus exists when moving from the global scale where current GCM's work best to the regional and local scale (i.e. Regional/river basin scales) where climate change predictions are necessary for impact assessment.

In this work, the CCCma CGCM1 50-kPa synoptic data were used for precipitation downscaling for the periods of 1962-85 and 2021-50. Temperature data were also interpolated for the period of 2021-50 using this model.

2.3 Precipitation Downscaling

In the present context, it is important to note that no GCM can fully consider the role of topography in the climate of the western Canadian Prairies. The topography of the CCCma CGCM1 includes a simple, smoothed version of the western cordillera, but the grid-point spacing is too coarse (Clausen and Roth, 1998; Venugopal et al. 1999; Kidson and Thompson, 1998) to be able to model the details of the strong rain-shadow

effects generated by the Rocky Mountains. Most GCM simulations have spatial resolutions (grid cells) on the order of several hundred kilometers. At these scales various GCMs tend to be somewhat consistent in terms of predicted changes in mean annual precipitation. Deficiencies exist in the detailed description of precipitation in climate models and numerical weather prediction models. Therefore it is necessary to develop precipitation downscaling techniques (Clausen and Roth, 1998; Venugopal et al. 1999; von Storch, 1995; Barry and Perry, 1973). Downscaling (discussed below) allows interpretation of the impact of climate change or climate variability on water resources management, which requires information at scales much smaller than the current resolution of regional climate models (Venugopal et al. 1999).

"Downscaling" is based on the view that regional climate is conditioned by climate on a larger scale, for instance continental or even planetary scales (von Storch, 1995, 1996a). Information is cascaded "down" from larger to smaller scales. Classification of atmospheric pressure-surface patterns is a fundamental practice in synoptic climatology (Barry and Perry, 1973). Simplifying the circulation into finite, yet representative map patterns enables investigators to relate atmospheric flow to the surface environment. The regional climate is the result of interplay between the atmospheric and oceanic, circulation and of region specifics, controls such as topography, land-sea distribution and land-use. Empirical/statistical downscaling seeks to derive the local scale information from the larger scale through inference from the cross-scale relationships, using a random or deterministic function *f* such that:

$$\textit{local climate response} = f(\textit{external, larger scale forcing})$$

The confidence that may be placed in downscaled climate change information is foremost dependent on the validity of the large-scale fields from the GCM. Since different variables have different characteristic spatial scales, some variables are considered more realistically simulated by GCMs than others. For instance, derived variables (not fundamental to the GCM physics, but derived from the physics) such as precipitation are usually not considered as robust information at the regional and grid scale (e.g. Osborn and Hulme, 1997; Trigo and DaCamara, 2000). Conversely, tropospheric quantities like temperature and geopotential height are intrinsic parameters of the GCM physics and are more skillfully represented by GCMs. However, there is no consensus in the community about what level of spatial aggregation (in terms of the number of grid cells) is required for the GCM to be considered skillful. For example Widemann and Bretherton (1999) find monthly precipitation on spatial scales of three grid lengths (in their case: 500 km) reliably suitable. For the purposes of this study, temperature and geopotential 50-kPa data were used from the GCM.

In order that the established GCM models generate reliable precipitation projections, we must ensure that GCM predicted large-scale variables under altered climate are reliable. To account for the systematic component of GCM internal errors, the ratio of GCM $2xCO_2$ (doubling point) and $1xCO_2$ was used as the predictor instead of direct $2xCO_2$ output.

The synoptic downscaling approach empirically defines weather classes related to local and regional climate variations. These weather classes may be defined synoptically or fitted specifically for downscaling purposes by constructing indices of airflow (Conway et al. 1996). Weighting the local climate states with the relative frequencies of the weather classes then derives the mean, or frequency, distributions of local or regional

climate. Climate change is then estimated by determining the change in the frequency of the specific weather classes.

Feedback and interactions in the climate system operate over a variety of temporal and spatial scales, such that it is difficult to treat any single component of the system in isolation. For large areas of the extra-tropics, however, numerous studies have demonstrated that the synoptic atmospheric circulation is a major factor influencing short-term climate variability at the regional and local scale (Hewitson and Crane, 1992). Studies for parts of North America show strong relationships between circulation and regional climate, with specific patterns of atmospheric circulation giving rise to characteristic precipitation and temperature anomalies (Klein and Klein, 1984, 1986; Yarnal and Diaz, 1986). Hay et al. (1991) used daily weather types (synoptic patterns) to simulate average precipitation, extreme precipitation, and drought conditions in the Delaware River Basin.

An interesting by-product of empirical downscaling approaches is that they offer a straightforward method of testing GCM's ability in simulating regional and local details. Specifically, are they able to reproduce the empirical links between large-scale and small-scale climate (Busuioc et al. 1999; Murphy, 1999; Murphy, 2000; Osborn et al. 1999).

2.3.1 Types of Downscaling

Manual:

Manual classification is familiar to most synoptic climatologists (Frakes and Yarnal, 1997; Wilby, 1995)). In this method, investigators subjectively classify the atmospheric continuum into a number of map-pattern categories. There are several well-

known regional manual classifications, such as the Lamb Weather Types for the British Isles (Lamb, 1972) or the Muller classification for the USA Gulf Coast (Muller, 1997). For this study we used synoptic classifications by Changnon et al. (1993) for Western North America.

Manual classifications are useful, but have significant drawbacks (Yarnal, 1993). They are conceptually straightforward, and therefore easier for non-climatologists to understand. Only climatologists, however, should carry out this process. Most classifications are unique and tailored to the specific research or region (Yarnal and Frakes, 1996; Wilby et al. 1994). For the purpose of this study a set of manual classifications previously outlined for western North America was used. Manual classification was the easiest and most efficient way to produce results, as previous experiments had been done.

An important strength of manual classification is the omnipotence it grants to the investigator (Frakes and Yarnal, 1997). Through prolonged contact with the data, he or she develops an intuitive understanding of the regional climate system. Further, while maintaining a regional focus, the investigator is free to expand the spatial and temporal window of observation, integrating knowledge of past and future weather conditions up and downstream.

This process, however, is quite tedious and time consuming, making replication of the classification less likely. Unless an existing, generic manual classification exists for a given region, the tedious, intensive nature of the work generally limits new projects through time constraints (Frakes and Yarnal, 1997).

Computer-based Classifications:

The alternative to manual classification is computer based. One of the most popular is the correlation-based method (Lund, 1963; Kirchhofer, 1973). The reason for this popularity is that it is essentially a computerized pattern-recognition algorithm. Time spent on getting the first classifications can be duplicated perfectly in minutes. As well, adjustments or even new correlation-based classification can take minutes to a few hours to perform (Frakes and Yarnal, 1997). The Kirchhofer technique for analyzing lattice data standardizes observed values at each location based on normalization scores. The lattice of normalized value is compared with other lattices to calculate a summary Kirchhofer score. The score is used to classify daily synoptic patterns. Further detailed information about this method can be found in Kirchhofer (1973) and Kaufmann et al. (1999).

A number of authors (Key and Crane, 1986; Yarnal and White, 1987, Yarnal et al. 1988; Huth, 1996) have demonstrated that the results of these schemes are highly subjective and that the number of synoptic types and days classified vary with a number of investigator-controlled variables. One of the biggest complaints is that the investigator cannot control the patterns generated. The number and size of groups identified by the Kirchhofer technique depends on the threshold and minimum group size (Key and Crane, 1986). There are no criteria to choose these parameters. As a result, analysts cannot be sure whether the synoptic patterns identified by the Kirchhofer technique represent groups that are generated by a meaningful meteorological phenomena or whether they emerge due to random change. Patterns can be easily missed; configurations with little climatic significance are often present; and the expertise of the investigator does not enter

into the classification process. Investigators do not become as familiar with the data they are working with (Frakes and Yarnal, 1997).

2.4 MTCLIM: A Mountain Microclimate Simulation Model

MTCLIM was developed by the Intermountain Research Station (Ogden, Utah), as a means of generating climate data for use in fire models, ecological models, insect and disease models, or aiding in the development of silviculture prescriptions (Hungerford et al., 1989). The discussion to follow regarding the MTCLIM Model follows the description from its manual, "MTCLIM: A Mountain Microclimate Simulation Model (Hungerford et al. 1989).

The MTCLIM model predicts daily solar radiation, air temperature, relative humidity, and precipitation for various mountainous sites by extrapolating data measured at (BASE) Weather Stations. In MTCLIM terminology, the location to be simulated is referred to as the SITE and the station for which records exist is known as the BASE. Data are corrected for the differences in elevation, slope, and aspect between the BASE station and the site. Data for the base weather stations are compiled giving daily air temperature, dewpoint, precipitation, radiation and variables other variables.

A flowchart of the model components of MTCLIM is shown in Figure 4.2. Input requirements are daily maximum and minimum temperature and precipitation, and dewpoint (if available) from the BASE station. At the SITE location the following variables are also needed: elevation, aspect, slope (percent), LAI (Leaf Area Index), isohyet (precipitation), east and west horizons, and albedo. Site factors are also needed for the site to which meteorological data are to be extrapolated to. These site factors and base station data are used by MTCLIM to predict incoming shortwave radiation, site air

temperature, site humidity, and precipitation. Wind conditions are not considered because extrapolation in mountains is not meaningful. However in Chapter 4 a wind variable is introduced as part of the vapour transfer modeling process.

Below is a description of each of the output variables from the MTCLIM Model for the SITE: Solar Radiation, Air temperature, Humidity, Precipitation.

Solar Radiation:

Incoming solar radiation is calculated by using an algorithm that relates diurnal air temperature amplitude to atmospheric conditions. First clear sky transmissivity is computed for the elevation of the site of interest, assuming clear sky transmittance at mean sea level is 0.65, and increasing by 0.008/m of elevation. Final atmospheric transmissivity is then calculated as an exponential function of diurnal temperature amplitude of the BASE station. This accounts for clouds, water vapour, pollutants, and other atmospheric factors reducing clear sky transmissivity. The equations for calculating daily solar radiation are extremely complex.

Air Temperature:

MTCLIM calculates three air temperatures for each SITE: daily maximum, daily minimum, and daylight average temperature. Daylight average temperature represents the temperatures over the daylight hours. It is assumed that the daily minimum temperature occurs near sunrise, and daily maximum temperature around midday. The model utilizes a sine wave to approximate the daylight average temperature. Daylight average temperatures are corrected for elevation using an environmental lapse rate of 6.4°C/1000 m, reduced by 10% on clear days and increased by 10% on cloudy days.

Air temperature on a south-facing slope increases and decreases on a north-facing slope relative to a flat surface at the same elevation due to the difference in radiant energy inputs. LAI is also taken into consideration when calculating temperatures, as the exchange of energy changes, due to canopy absorption.

Relative Humidity:

SITE humidity is derived from BASE station dewpoint and simulated SITE daylight average temperature. Where the recorded dewpoint is not available for the BASE, night minimum temperature is assumed to be representative of the dewpoint temperature. SITE dewpoint is either measured or estimated from the base station minimum temperature, and then corrected using a lapse rate of 2.7°C/1000m, modified to account for radiation (Finklin, 1983).

Precipitation:

Given the highly variable nature of mountainous precipitation, accurate simulation is not possible, especially at shorter time scales. For this reason, MTCLIM uses a simplified algorithm that applies the ratio between BASE to SITE annual average precipitation to the daily BASE station values. SITE annual precipitation is estimated from annual isohyet maps while BASE station annual precipitation is obtained from long-term averages for the BASE stations used. Sheppard (1996) derived these precipitation values.

2.4.5 Other MTCLIM Inputs

Input requirements include terrain features, vegetation characteristics, and meteorological information for the SITE of interest. For the BASE, requirements include basic terrain features and meteorological information only. These variables plus several others relating to temperature and dewpoint lapse rates, enable MTCLIM to output simulated daily values for solar radiation, temperature, relative humidity, and precipitation.

Physiographic features required for all grid cells include elevation, slope, aspect, and east-west horizon angles. Vegetation characteristics include LAI and the associated albedo (albedo represents the percentage of solar radiation reflected by a surface). The LAI is a value which describes the leaf area per square metre of ground surface. Hungford et al. (1989) use an LAI of 1.0 and suggest it as being appropriate for a Northern Rocky Mountain coniferous forest. Forest canopies reflect approximately 10-20%, grass 20-25%, and rock about 10-30% of incoming radiation back into the atmosphere. Given these estimates, it can be assumed that remaining incoming energy is absorbed.

2.4.6 MTCLIM Model Output

MTCLIM output consists of the simulated microclimate for a single SITE based on the data from one or two nearby weather recording stations. The data consists of: daily total solar radiation in kilojoules per metre squared (kJ/m^2); daily average temperature, daily maximum temperature, daily minimum temperature (^oC); Relative humidity (%) over the daylight hours; total daily precipitation (mm).

2.5 SIMGRID Model

The MTCLIM model predicts a number of variables for one site at a time, which can be very time consuming when trying to calculate a number of different areas. SIMGRID (Sheppard, 1996) was developed based on the same input and output variables as MTCLIM, but simulates output for more than one pixel at a time. For the purpose of this study SIMGRID is used to calculate data for 144 558 pixels, each 100m x 100m, covering an entire watershed in area of 1445 km^2.

2.5 Over-winter Snow Balance

Snow accumulation account for up to 85% of runoff in western North America (Grant and Kahan, 1974). In the arid and semi-arid prairies most runoff is snowmelt. Snow melt runoff occurs because the soil is frozen and very little infiltration is possible (Xiuqing et al. 2001).

Snow that accumulates over the winter period changes in structure and form. Four factors affecting snow pack conditions are:

- Settling due to gravity
- Compression due to wind action
- Freeze/melting cycles
- Moisture/heat fluxes due to rain, condensation, or sublimation

Snow accumulation is highly variable, generally with greater accumulations at higher elevations. Aspect is also an important factor in snow accumulation, due to the effect of radiation. North facing slopes receive the least amount of. Vegetation is important, as it slows wind movement and blocks radiation. A good understanding of the

elevational distribution of snow cover is necessary to predict the timing and volume of runoff. In a complex mountainous terrain the snow cover distribution within a watershed is highly variable in time and space and is dependent on elevation, slope, aspect, vegetation type, surface roughness, radiation load, and energy exchange at the snow-air interface.

Sublimation or condensation/freezing may also be occurring. These processes depend upon: wind speed; humidity (dew point); temperature; and radiation input.

The amount of runoff available in any given year is largely determined by the amount of precipitation received in the previous winter, so an understanding of precipitation patterns is important in gauging future water supplies (Bohr and Aguado 2001). Much research has been performed in this region over the past several decades relating winter precipitation to elevation, aspect, global atmospheric circulation, and a variety of other factors (e.g., Caine, 1975; Changnon et al. 1991, 1993; McCabe, 1994; Johnson and Hanson, 1995).

Researchers have typically used the April 1 snow water equivalent (SWE) as a surrogate for the amount of precipitation received in a season (e.g., Changnon et al. 1991, 1993; McCabe, 1994; Cayan, 1996). Specifically, they assumed that the April 1 SWE is strongly indicative of both the total amount of cold season precipitation as well as the peak snowpack of the season. The April 1 SWE appears to provide a more accurate estimation of the total seasonal precipitation over the long term (Bohr and Aguado, 2001). April 1 SWE can be used as an index for both peak SWE and total cold season precipitation, as April 1 snowpack correlates very strongly with both of these variables (Bohr and Aguado, 2001).

Under climate warming, April 1 may no longer be significant for this measurement, as warming temperatures will shorten the winter season. Brubaker and Rango (1996) indicated that in mountainous regions a warmer climate is expected to cause earlier snowmelt with decreasing summer runoff. Leith and Whitfield (1998) studied streams in south-central B.C. for hydrological changes that might be caused by climate change. In the late-fall and early-winter, warmer temperatures would result in more precipitation as rain rather than snow. Due to the fact that a portion of the rainfall would produce runoff, the overall streamflow of this season would increase. These higher late-fall/early-winter streamflows would result in earlier spring runoff and a reduced streamflow in the subsequent summer months (Leith and Whitfield, 1998).

2.6.1 Vapour Transfer Model

The rate of sublimation is determined by the temperature and humidity gradients across the boundary layer between each snow particle and its environment. The rate of vaporization is determined by the balance between heat transferred to the particle and water vapor removed from the particle boundary layer (Schmidt, 1972).

Blowing snow can strongly influence the water budget in regions with seasonal snowcovers, through the transport and redistribution of snow by wind and the sublimation of airborne snow while in motion (Dery et al. 1998). Although much research on the movement and drifting of snow has been conducted (e.g. Kind, 1981; Schmidt 1982), it is only recently that the potentially significant impact of blowing snow sublimation on the water budget of high-latitude regions has attracted wider interest. Dyunin et al. (1991) state, for instance, that the deforestation of northern lands may lead inevitably to their aridization as the wind is now capable of transporting snow out of the

regions and stimulating the sublimation of blowing snow. Pomeroy and Gray (1994, 1995) have argued that the transport of snow in prairie fields may remove as much as 75% of the annual snowfall over a one kilometer long fallow field, with about half of this amount sublimating into the atmospheric boundary layer (ABL).

In this study a vapour transfer model developed by Thorpe and Mason (1966) and modified by Dery et al. (1998) was adopted. This model looks at the four main variables which effect vapour transfer: radiation, wind, relative humidity, and air temperature. Although it looks very complex it is much like the simple Meyer lake evaporation equation (Singh 1992):

$$E = f(u)\,(e_s - e_d)$$

where E is the evaporation rate, f(u) is a function of wind speed u, and e_s-e_d is the saturation vapour-pressure deficit. Thus, evaporation is related to wind speed and is proportional to the vapour-pressure deficit, which is the difference between the saturated vapour pressure at the water-surface temperature (e_s) and the vapour pressure of the air at some height above the ground (e_d) (Singh, 1992).

Evaporation/sublimation/condensation requires a vapour pressure difference between the surface and the overlying air, and wind generated turbulence. During snowmelt, atmospheric vapor pressure increases with rising temperature while the snow-surface is constrained to the saturation vapour pressure at 0^{o}C. Stable atmospheric stratification becomes the norm. As the season progresses, atmospheric vapour pressure may exceed that of the snow-surface, producing condensation. Wind speed is a critical variable; all of the fluxes are directly proportional to wind speed (Leydecker and Mulack, 1999).

The change in mass (kg) of a blowing snow particle of radius r (m) due to sublimation per second is given by (Thorpe and Mason, 1966):

$$\frac{dm}{dt} = \left(2\pi r\sigma - \frac{Q_r}{KN_{Nu}T_a}\left[\frac{L_s}{R_vT_a} - 1\right]\right) \Big/ \left(\frac{L_s}{KN_{Nu}T_a}\left[\frac{L_s}{R_vT_a} - 1\right] + R_v\frac{T_a}{N_{Sh}De_i}\right) \qquad (2.1)$$

where:

$2\pi r$ = area function of snow particle (m)

σ = (dimensionless and negative) water vapour pressure deficit with respect to ice $((e - e_i)/ e_i)$, where e and e_i are the actual and saturation vapour pressures at air temperature T_a.

$Q_r = \pi r^2(1 - \alpha_p)Q_*$, net radiation transferred to the particle Q_r (W), (Schmidt,1991)

α_p = shortwave particle albedo (0.5) (Schmidt et al., 1998)

Q_* = total incident radiation (W m^{-2})

K = thermal conductivity of air (2.4 x 10^{-2} W m^{-1} K^{-1})

N_{Nu} and N_{Sh} = $1.79 + (0.606\ N_{Re}^{0.5})$ (Nusselt and Sherwood numbers)

$N_{Re} = (2rV_r/\upsilon)$ (Reynolds number)

V_r = ventilation velocities (Schmidt, 1982; Dery and Taylor, 1996). Horizontal particle velocity components are assumed equal to the horizontal wind speed

υ = kinematic viscosity of air (1.53×10^{-5} $m^2 s^{-1}$) (Dery and Yau 1999)

T_a = ambient air temperature (Kelvin)

L_s = latent heat of sublimation (2.838 x 10^6 J kg^{-1})

R_v = gas constant for water vapour (461.5 J kg^{-1} K^{-1})

D = molecular diffusivity of water vapour in air (2.25 x 10^{-5} m^2 s^{-1})

From the rate of mass loss by sublimation (Eqn 2.1) per snow particle one can determine the rate of loss from a unit area by determining the number of particles per unit volume (# particles/m^3) N(z). However, the number of snow particles in a cubic metre depends on the particle shape (α) and radius (r_m). In the saltation layer, it is common to assume $\alpha = 5$ and that r_m, the mean particle radius, is 100 μ m (Pomeroy, 1998) although variation in these parameters can be expected with changing environmental conditions. Where $\alpha = 5$, (Dery et al., 1998) the threshold for transport is $N(z) = 9.09 \times 10^7$ m^{-3}.

Hence, by knowing the rate of sublimation per snow particle and the number of particles within a cubic metre of snow we can determine the overall sublimation of a snowpack.

$$Q_{subl} = \frac{dm}{dt} * N(z) \qquad (2.2)$$

Where:

Q_{subl} (kg m^{-2} s^{-1}) = total sublimation rate for a column of blowing snow over a unit horizontal land surface,

$\frac{dm}{dt}$ = change in mass (kg) of a blowing snow particle of radius r (m) due to sublimation per second,

$N(z)$ = number of snow particles per unit volume (# particles/m^3),

We can calculate the overall sublimation of a snowpack if the approximate number of particles within a cubic metre of the saltation layer are known or estimated as above.

2.6.2 Snowpack Melt

The estimation of snowpack accumulation and melting is accomplished through an over-winter snow accumulation/ablation model, which incorporates the snowmelt algorithm from the UBC Watershed Model (Pipes and Quick, 1977) and an empirically-based accumulation model that describes the composition of precipitation based on temperature (Wyman 1995), and the vapour model applied here.

The UBC snowmelt technique takes into consideration three primary sources of snow melting energy. The first of these, convective heat transfer from warm air, is estimated as being equal to the mean daily temperature above freezing. Second, the net radiant energy gains from shortwave and longwave radiation exchanges is considered. It is represented simply as the daily temperature range. Finally, the latent heat gain from condensation or loss through evaporation at the surface is derived as a function of the range of temperatures.

Snowmelt is dependent upon the ability of the snowpack to store cold. Pipes and Quick (1977) take into account a negative melt decay function in their cold storage equation which serves to limit the effect of daily temperature conditions to the previous ten days. The following is referred to as the negative melt formula:

$$TREQ_i=(ANMTLF^* TREQ_{i-1}) + TMEAN_i$$

where:

$TREQ_i$ and $TREQ_{i-1}$= snowpack cold storage on days i and i-1,
ANMLTF = the decay of constant (set to 0.85),
$TMEAN_i$ = the mean daily temperature on day i,

In order for melt to occur, the snowpack's cold storage must first be exhausted, when this happens open area melt takes place according to the following formula:

$$MELT_i = PTM * (TMAX_i + TCEADJ * TMIN_i)$$

where:

$MELT_i$ = melt depth in millimeters of water equivalent on day i,
PTM = point melt factor in millimeters per day per $^{\circ}C$ (Pipes and Quick give a PTM = 3, a value of 1.8 is recommended by Wyman, 1995, and Byrne, 1990 used 1.0 for the prairies.),
$TMAX_i$ = daily maximum temperature on day i,
$TMIN_i$ = daily minimum temperature on day i,
TCEADJ = the energy partition multiplier,

and where:

$$TCEADJ = \frac{TMINi + T_r/2}{XTDEWP + T_r/2}$$

T_r = range of temperature over the particular day,
XTDEWP = reference dewpoint that control energy partitioning between melt and sublimation (set to $18^{\circ}C$),

If falling precipitation is in the form of snow and temperatures are insufficient for melt to take place, then it is likely that existing snowpack will increase. The following formula describes the criteria by which the distinction is made between precipitation that falls as snow and that which falls as rain (Wyman, 1995).

Daily snow water equivalent (SWE):

$$SWE = PPT_n - RAIN_n$$

where:

SWE = precipitation that falls as snow on day n (mm),
$RAIN_n$ = precipitation that falls as rain on day n (mm SWE),
PPT_n = total daily precipitation on day n (mm SWE),

and where:

$RAIN_n = 0$ if mean daily temperature < 0.6°C,
$RAIN_n$ = PPTn * (TMEANn/3 – 0.2) if mean daily temperature > 0.6°C and < 3.6°C,
$RAIN_n$ = PPTn if mean daily temperature > 3.6°C,
$TMEAN_n$ = mean daily temperature on day n.

In the basic equation, total snow on a given day, SWE, is defined as the total daily precipitation minus the amount of precipitation that falls as rain. The amount of rain on a given day, RAIN, is dependent upon, TMEAN. When TMEAN is less than 0.6°C, RAINn = 0 because all precipitation is considered to be in the form of snow. When TMEAN is greater than 3.6°C, $RAIN_n$ = the total daily precipitation, because all precipitation is considered to be in the form of rain. The case of TMEAN falling between 0.6 and 3.6 °C is slightly more complex since the total daily precipitation is assumed to be a mix of snow and rain, the ratio of which is determined by the formula:

$$RAIN_n = PPT_n * (TMEAN_n/3 - 0.2)$$

The form precipitation takes determines the manner in which Wyman (1995) deals with its impact on the snowpack. Obviously, the addition of snow causes an increase in the depth of snow water equivalent held in the pack. The addition of rain,

however, may do one of two things: 1) When the total rain added is less than that which the snowpack is capable of absorbing, the pack becomes more dense but no runoff occurs. 2) When the total rain added exceeds the pack's capacity to absorb water, additional rain and surface melt propagates through the pack where it contributes to runoff.

Chapter 3

Linking GCM synoptics and precipitation for western North America

3.1 Introduction

A key issue in forecasting future water supplies from alpine areas in western North America is predicting future winter precipitation scenarios under forecast climate warming. Spring runoff is important in western North America for agriculture (irrigation), ecosystem protection and human consumption. Nearly 85% of the area's total annual streamflow is derived from the snowpack (Grant and Kahan, 1974), thus is it important to understand the fluctuations in winter precipitation that may occur due to global warming. A better understanding of winter climate variability will impact policy decisions concerning water resource management and will aid in anticipating extreme events.

Global Circulation Model (GCM) precipitation output is typically unreliable on the regional and local scales for hydrological analysis (Saunders et al. 1994; von Storch et al. 1993). The horizontal resolution of present day coupled GCM's is still in the order of hundreds of kilometers, hence current techniques such as synoptic downscaling from GCM's have been adopted to further refine local and regional scale monthly or seasonal precipitation scenarios (Byrne et al. 1999; Konrad, 1997; Krichak et al. 2000).

Atmospheric circulation patterns govern the climatic conditions during the winter season in western North America. Previous studies (e.g. Byrne et al. 1999; Latif and Barnett, 1996; Trenberth, 1990; Yarnal and Diaz, 1986) have documented variability in these atmospheric circulation patterns over space and time, and have shown the linkages between the variations in synoptic pattern frequency/duration and winter precipitation. Policymakers and stakeholders are interested in the effects of climate variability at

regional and local scales (Giorgi and Mearns, 1997) hence much research has been conducted in the area of climate downscaling. These studies attempt to identify the effects of large-scale spatial and temporal climate fluctuations on small scale geographic regions (e.g. Hewitson and Crane, 1996; Cavazos, 1997) with the objective of carrying out integrated regional assessments of climate variability and change; and finally, defining the eventual physical and socioeconomic impacts (Easterling, 1997).

Changnon et al. (1993) defined seven dominant synoptic flow patterns (Figure 3.1) for western North America for the period of October 1950 to March 1985. These synoptic patterns control the spatial distribution/volume of winter precipitation in the Rocky Mountain States. A GCM that effectively replicates historical frequencies of these seven patterns can be utilized to develop future precipitation scenarios. A previous study (Byrne et al. 1999) used the CCCma GCM2 1992 model run with good results. However, this model is now outdated and has been superceded by the more comprehensive Canadian Centre for Climate Modeling and Analysis (CCCma) First Generation coupled general circulation model (CGCM1).

In this chapter, winter (October through March) precipitation scenarios were developed using synoptic downscaling techniques based on output from the CGCM1. Precipitation scenarios were developed for five climate stations in diverse locations in western North America (Figure 3.2), under climate warming conditions.

3.2 Methodology

The seven historical winter upper air synoptic patterns defined by Changnon et al. (1993) were adopted for our analysis of the CGCM1. Changnon et al. (1993) found three basic and persistent patterns of snowpack values:

- years with a consistent anomaly over the entire region (wet or dry years),
- years with a distinct north to south gradient, and
- average years,

The CCCma CGCM1 model simulates climate conditions for 48 latitude by 96 longitude grid points on a 3.75° by 3.75° Gaussian grid with 10 vertical levels (Flato et al. 2000). Three available simulations have been run for three 200-year (1900-2100) transient simulations (Boer et al. 2000). Transient simulations assume a steady rate of CO_2 increase in the atmosphere over time. The three available simulations are (CCCma 2000):

- Control: greenhouse gas concentrations and other external forces of change were held constant at present day concentrations.
- GHG: considers only increases in greenhouse gas concentrations at a rate of 1% per year from the observed 1900 until the year 2100, converted to an equivalent concentration of carbon dioxide.
- GHG + A: the effects of greenhouse gases and an additional factor, the direct effect of sulphate aerosols.

For the purpose of this study the GHG + A simulation was chosen. Atmospheric concentrations of greenhouse gases and aerosols in GHG + A correspond to historical concentrations from 1900 to present, and a CO_2 increase at a rate of 1% thereafter until 2100. The time of CO_2 doubling is approximately 2050 (Boer et al. 2000). The direct

effect of sulphate aerosols (A) is also included by increasing the atmospheric albedo (Reader and Boer 1997). The indirect effect of sulphate aerosols on the optical properties and lifetime of clouds was not included, since estimates of this forcing effect are highly uncertain (IPCC 1996).

Arc Macro Language (AML) routines were developed to import the daily CGCM1 upper air data (50-kPa surface) for the years 1962 through 1985 for the months of October through March into ArcInfo desktop GIS system (ESRI, 2001). The 50-kPA pressure elevation fields were analyzed using a grid raster with 30 metre elevation intervals. The location(s) of the principal westerly jet (the zone of greatest wind velocity) were defined by visual inspection of the daily elevation fields. The zone of greatest contour density was defined as the core of the westerly flow - i.e. steep elevation gradients are assumed to represent the mid latitude jetstream. The daily pattern displayed over North America on the screen was compared to each of the seven patterns described by Changnon (1993). The screen pattern was assigned to whichever pattern type it most closely resembled. Patterns not clearly resembling any of the seven patterns types were assigned as unclassified. For the $1xCO_2$ data, about two percent of the days were unclassified. For the $2xCO_2$ data, less than one percent of the days were unclassified. Therefore, we assume any effects of unclassified days to be negligible and in the analysis we only use the statistics for the seven patterns. This assumption is supported by the nature of the pattern form on unclassified days where the jet stream effectively disappears, indicating no meaningful synoptic control on weather (precipitation) on those few days.

In this chapter the CGCM1 model output was selected for the years 1960-85 to represent historical conditions ($1xCO_2$) conditions. This period represents a time frame

of minimal increases of CO_2 concentrations in the atmosphere. For the warmed period, the 2021-50 time frame was selected representing an approximate $2xCO_2$ atmospheric condition.

The Changnon et al. (1993) and CGCM1 historical (1962-85) pattern frequency data must display similar distribution characteristics and central tendencies before the model can be considered valid in representing present and future scenarios. Independent t-tests and Kolmogorov-Smirnov (K-S) tests were conducted between the CGCM1 historical and Changnon frequency data to determine whether the $1xCO_2$ (1962-85) output accurately simulated the pattern types and occurrence frequencies reported by Changnon et al. (1993). The same visual classification technique was used to evaluate the pattern types and frequencies under a $2xCO_2$ climate scenario (2021-50).

Winter precipitation accumulations (October 1 to March 31) for five geographically diverse mountain locations in western North America (Figure 3.2) were linked to the Changnon et al. (1993) dominant synoptic pattern frequencies, using stepwise linear regression for the 1951-85 $1xCO_2$ data series. These sets of pattern frequencies are significant predictors of winter precipitation accumulations for this series. These models were assumed to also be true under $2xCO_2$ conditions.

The linkage between winter synoptic patterns and precipitation for five mountainous locations: Lake Louise, Alberta; West Glacier, Montana; Steamboat Springs, Colorado; Yreka, California; and Moran, Wyoming were determined using historical daily precipitation and the historical pattern type frequency data of Changnon et al. (1993) using statistical analysis (no-intercept stepwise multiple linear regression) in SPSS.

3.3 Results

Using the CGCM1 to forecast future conditions requires that the model demonstrate reasonable ability to replicate historical conditions. Hence we compared the CGCM1 $1xCO_2$ pattern frequency distribution to the historic Changnon et al. (1993) frequencies. Presuming the CGCM1 accurately portrays the historical frequencies, validity of the $2xCO_2$ frequency distribution may then assume. Any substantive changes in the 1x and $2xCO_2$ frequencies represent likely changes in future synoptic conditions; and hence linkages between precipitation and synoptic frequencies may be used to develop future precipitation scenarios.

The comparison of the Changnon (1993) historical synoptic and $1xCO_2$ synoptic frequency distributions is presented in Tables 3.1 and 3.2. The differences in both central tendencies and distributional characteristics for the annual frequencies of each synoptic type were tested using an independent sample t-test and Kolmogorov-Smirnov (K-S) test respectively. In order to determine that the model is sufficiently representing historic data, the overall pattern frequency distributions and means must have a $p > 0.05$, meaning no significant different exists. The data in Table 3.1 show that only one significant difference exists between the historical and $1xCO_2$ patterns (NWZ has $p = 0.048$ – note this only misses significance by .002). Hence the t-test reveals, for all intents and purposes, that the central tendencies of the pattern frequencies from the CGCM1 $1xCO_2$ period are similar to those of the historical data. The "near" significance of the NWZ pattern does not alter the analysis – NWZ occurs only about four percent of the time. Hence, the NWZ pattern does not substantively influence precipitation in our study region.

The K-S test results (Table 3.2) reveal that there are no significant differences between the frequency distribution characteristics for all $1xCO_2$ model data when compared to the historical data.

There are significant changes in synoptic pattern frequencies that occur in the $2xCO_2$ synoptic frequency distribution. Change is evident in the central tendencies (Table 3.3) and distribution characteristics (Table 3.4) for DR, NWW, SWT and SWC patterns.

Table 3.5 shows the actual differences in the average frequencies of each pattern between the CGCM1 $1xCO_2$ and CGCM1 $2xCO_2$ and the historical, 1951-85 Changnon et al. (1993) data. The ratio of changes ($2xCO_2/1xCO_2$) for DR, NWW, SWT and SWC are 2.22, 1.21, 0.75, and 0.38 respectively. These changes will be discussed in light of the statistical analysis presented below.

3.4 Linking synoptic frequencies to precipitation occurrence

No-intercept (forced origin) stepwise multiple linear regression techniques were utilized to develop a model to forecast future winter precipitation. A series of regression models were developed using historical precipitation data (Environment Canada, 1999; NCDC, 2000) and Changnon et al. (1993) historical synoptic data. The dependent variable in each model was the accumulation of annual wintertime precipitation (October through March) at a given climate station; and the independent variables were Changnon et al. (1993) synoptic pattern frequencies. For the historical analysis, daily precipitation data was available between 1951-85 (n=35) for each of the 5 stations chosen. Relationships between annual historical winter precipitation and historical synoptic type

frequencies were developed using stepwise regression to establish which combination of pattern type(s) affected winter precipitation values at each station (Table 3.6).

It is important to note that forced origin multiple regression was used to develop these models. Forced origin assumes that the dependent variable is zero in the absence of any effect from any or all of the independent variables. This is the case herein – the unclassified days would be the only variables that argue for a constant in the regression to account for unexplained variability. The unclassified days account for less than two percent of the cases. For this reason, we applied the forced origin model. This assumption makes climatological sense as well. Virtually all of the winter precipitation in alpine environments in western North America is under synoptic (orographic or convergent) control. Convective precipitation is minimal in winter.

The winter precipitation at Lake Louise, Alberta; West Glacier, Montana; and Yreka, California are all dominantly controlled by the NWW pattern. The winter precipitation at Steamboat Springs, Colorado; and Moran, Wyoming is controlled by the SWT pattern. One might have expected more than a single pattern to strongly influence precipitation at each station. However, for the purposes of this project, none of the models included more than one significant independent variable. These models therefore argue for local and regional control of precipitation by single synoptic pattern types. Similar results were found by Byrne et al. (1999), where spring runoff peaks in two major watersheds; the Upper Colorado River in Western Colorado; and the Oldman River in Southern Alberta; were significantly connected to only one synoptic pattern. It is important to note that in some cases, the regression statistics reported more than one significant independent variable. However, the inclusion of more than one independent variable made only trivial (approx. one percent) improvements in the model. For

example, for West Glacier, both NWW and SWT were significant variables in the regression model. However, the addition of SWT only improved the explanation of the variability by one percent. NWW accounts for ninety six percent of the variability. The simpler model was chosen for subsequent analysis.

3.4.1 Example of Precipitation Downscaling

Future winter precipitation values were developed using the step-wise regression equations previously described with adjustments to historical seasonal pattern frequency data as follows (Table 3.7):

For Steamboat Springs, CO., the regression equation (Table 3.6) for winter precipitation P as a function of historical pattern frequencies is

$$P = 13.05\ SWT$$

where SWT is the relative frequency of that pattern in any year. Hence for a year where SWT occurs 40% of the time, the winter precipitation for the year would be 522 mm. Under a $2xCO_2$ climate, SWT would decrease by one quarter of historical values (Table 3.5). In Table 3.7, column 2 is the average annual winter (October-March) precipitation for 1951-85. Column 3 is the average 2x CO_2 winter (October-March) precipitation for the same time period. To estimate the changes in winter precipitation the ratio between $1xCO_2$ and $2xCO_2$ SWT mean frequency were used to adjust the historical SWT data. Therefore, the precipitation for Steamboat Springs is calculated by:

$$P = 13.05 * SWT * (2xCO_2\ SWT / 1xCO_2\ SWT).$$

This same procedure was used to compute the average $2xCO_2$ winter precipitation for the remaining 4 climate stations.

3.5 Discussion

Significant differences in future precipitation amounts for the climate stations included in this analysis are revealed. Areas in which the NWW pattern is the driving force behind winter precipitation show increases in overall precipitation; and SWT-dominated areas show an overall decrease in precipitation.

Time series of annual changes in winter precipitation for historical and $2xCO_2$ conditions for each station are presented in Figure 3.3. The $2xCO_2$ precipitation values were calculated using the station regression equations defined in Table 3.6 and following the same ratio adjustments described above, except for the years 1951-80, where annual values were used instead of mean annual precipitation. Figure 3.3 indicates that there will be significant overall fluctuations in future precipitation. Those stations predominantly influenced by the NWW pattern could experience major increases in overall precipitation compared to those influenced by SWT, where major decreases are expected.

These precipitation values are not representative of snow accumulation. Temperature change must also be taken into consideration when converting estimates of precipitation into snowpack and into spring runoff volumes.

3.6 Summary

This study has adapted GCM downscaling analysis to develop winter precipitation scenarios for selected climate stations in western North America. The spatial characteristics of the CCCma CGCM1 were visualized within a GIS, and circulation patterns were visually classified into one of seven mutually exclusive 50-kPa wintertime

synoptic patterns described by Changnon et al. (1993). Historic synoptic pattern frequencies were found to explain at least 90% of the wintertime precipitation for the 5 climate stations chosen.

In order to determine whether the GCM was accurately displaying climate warming, the model had to be validated with historic pattern frequencies. The simulated $1xCO_2$ synoptic frequencies were compared to historical data, and the GCM model was found to be robust. Thus, reliability could be employed in the model for the forecasting of $2xCO_2$ scenarios. Pattern frequencies from $2xCO_2$ were compared to historic frequencies to determine which patterns were predicted to exhibit significant differences under a climate-warming scenario. An interpretation of these differences in synoptic flows points to considerably wetter conditions in the north and the west coast of the study area, and considerably dryer conditions in the central and southern areas of the study area.

Climate stations influenced by the NWW pattern (Lake Louise, West Glacier and Yreka) show an increase in winter precipitation of 40%. Stations controlled by the SWT pattern show a decline of about 30% in winter precipitation (Moran and Steamboat Springs). Winter precipitation is critical to spring runoff and seasonal water supply in the regions studied here.

This analysis provides a basis for the rapid prediction of future winter precipitation for most locations in western North America. The understanding of winter precipitation scenarios for western North America will be enhanced by expanding this type of analysis to a number of other locations and regions.

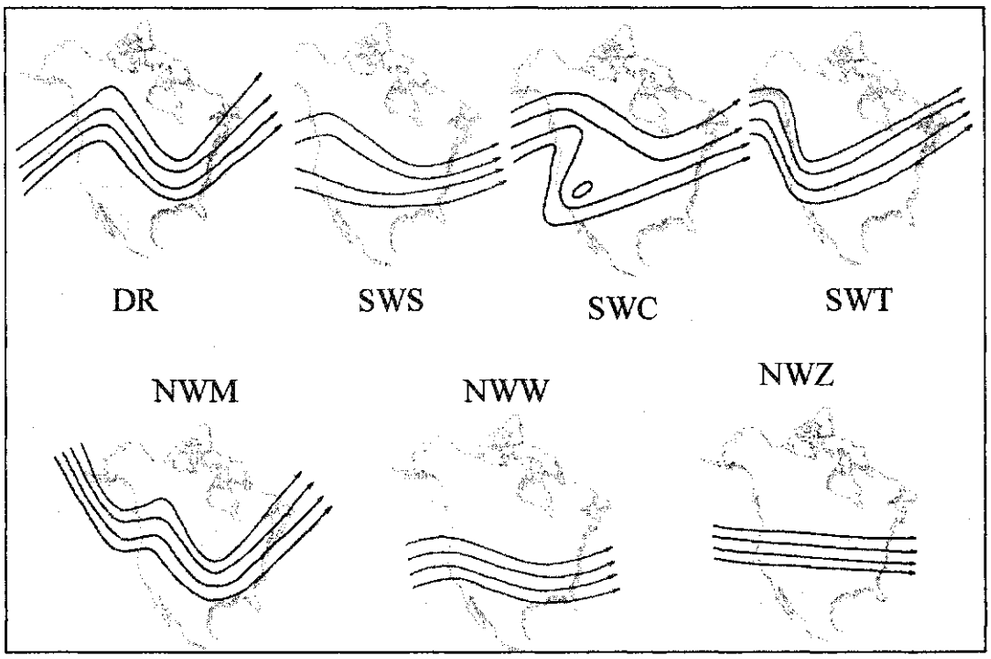

Figure 3.1 The seven dominant synoptic 50-kPa patterns as defined by Changnon et al. (1993). The ridge pattern (DR) is associated with dry anomalies over the entire region. The split-flow pattern (SWS) is associated with wet anomalies across southern regions. The cutoff pattern (SWC) is associated with wet anomalies across southern regions. The trough pattern (SWT) is associated with wet anomalies across southern regions. The meridional northwest pattern (NWM) is associated with wet anomalies across northern regions. The west-northwest pattern (NWW) is associated with wet anomalies across northern regions. The zonal pattern (NWZ) is associated with wet anomalies across northern regions.

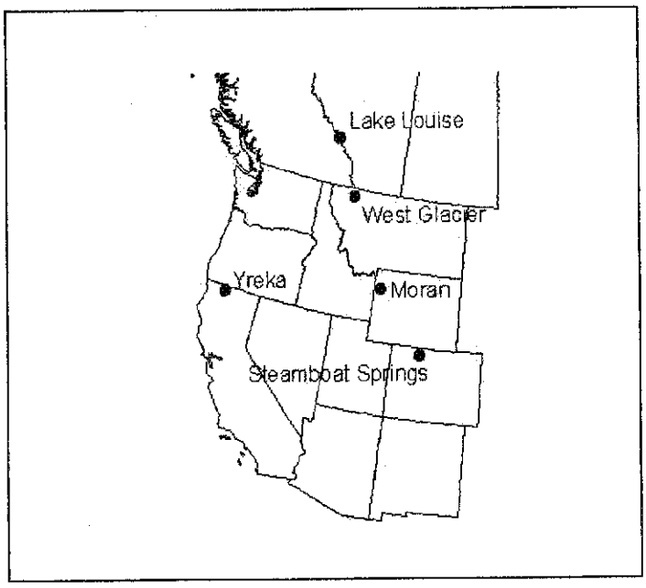

Figure 3.2 Location of 5 climate stations chosen, throughout western North America.

Table 3.1 Independent t-tests for differences in central tendency of $1xCO_2$ CGCM1 and Historical 50-kPa Pressure Fields ($p>0.05$, no significant difference)

	DR	NWM	NWW	NWZ	SWT	SWS	SWC
t	1.3	-0.077	1.034	-2.020	0.343	-0.432	0.044
p (two tailed)	0.204	0.94	0.306	0.048	0.733	0.668	0.965

Table 3.2 K-S Test for Differences in Distribution of $1xCO_2$ CGCM1 and Historical 50-kPa Pressure Fields.

	DR	NWM	NWW	NWZ	SWT	SWS	SWC
K-S, Z	1.271	0.665	1.262	1.253	0.584	0.818	1.105
p (two tailed)	0.079	0.769	0.083	0.086	0.885	0.516	0.174

Table 3.3 Independent t-tests for differences in central tendency of $2xCO_2$ CGCM1 and Historical 50-kPa Pressure Fields.

	DR	NWM	NWW	NWZ	SWT	SWS	SWC
t	5.606	-0.155	2.488	1.771	-4.694	-0.865	-8.725
p (two tailed)	0.00	0.878	0.016	0.082	0.00	0.391	0.00

Table 3.4 K-S Test for Differences in Distribution of $2xCO_2$ CGCM1 and Historical 50-kPa Pressure Fields.

	DR	NWM	NWW	NWZ	SWT	SWS	SWC
K-S, Z	2.438	0.834	1.483	1.161	1.815	0.950	3.024
p (two tailed)	0.00	0.490	0.025	0.135	0.003	0.328	0.00

Table 3.5 Average Annual Frequency for the Historical and $2xCO_2$ 50-kPa Synoptic Patterns (* Historical Frequencies for the period of 1951-85).

	DR	NWM	NWW	NWZ	SWT	SWS	SWC
Changnon	10.7	15.2	21.9	3.3	25.5	4.5	16.6
$1xCO_2$	13.2	15.1	18.6	4.0	26.0	4.2	16.7
$2xCO_2$	23.7	15.0	26.4	4.6	19.2	3.9	6.3

Frequency is given in percent. Annual values do not add up to 100% due to unclassified days.

Table 3.6 Multiple linear regression equations developed for predicting average winter precipitation amounts based on historical pattern occurrence for the 5 climate stations.
*Forced origin multiple regression analysis was used, thus the values of R^2 cannot be compared to those models which include a constant.

Station	***Regression Eqn.***	***R^2***	***Alpha***	***SE of Coef.***
Lake Louise	ppt = 16.476 NWW	0.92	p<0.05	0.848
West Glacier	ppt = 18.67 NWW	0.959	p<0.05	0.695
Steamboat Springs	ppt = 13.05 SWT	0.925	p<0.05	0.667
Moran	ppt = 14.132 SWT	0.934	p<0.05	0.653
Yreka	ppt = 16.872 NWW	0.908	p<0.05	0.962

Table 3.7 Comparing1951-85 winter precipitation amounts (mm), October through March, for the 5 stations under historical (actual ppt) and 2xCO_2 conditions, based on multiple linear regression equations.

	Historical(1951-85)	Adjusted 2xCO2
Station Name	**mm**	**mm**
Lake Louise	376	534
West Glacier	429	609
Steamboat Springs	338	250
Moran	365	270
Yreka	389	552

a. Lake Louise,Ab

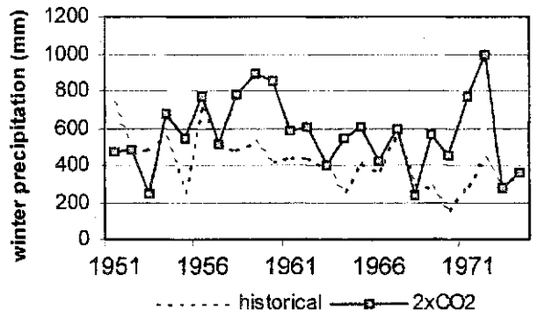

b. Steamboat Springs, Co

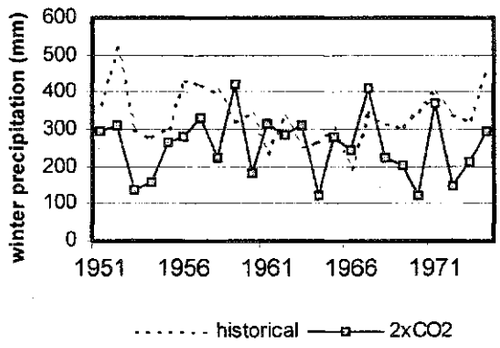

c. Yreka, Ca

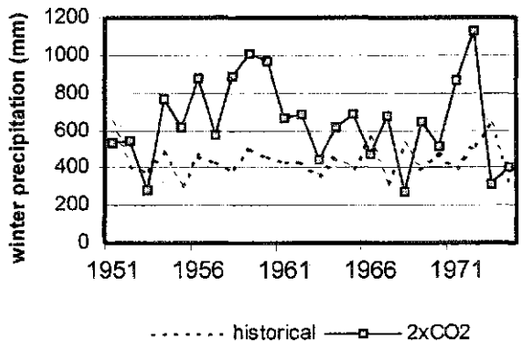

d. West Glacier, Mt

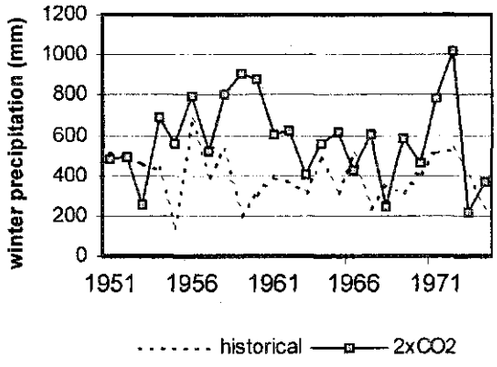

e. Moran, Id

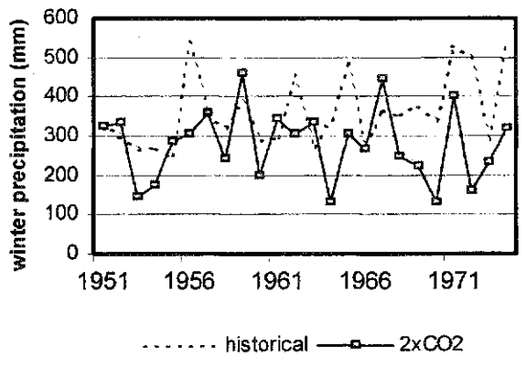

Figure 3.3 Historical and $2xCO_2$ forecast changes in winter precipitation (mm) for five climate stations. a. Lake Louise, AB. b. Steamboat Springs, CO. c. Yreka, CA. d. West Glacier, MT. e. Moran, ID.

Chapter 4

Climate Warming Impacts on Snowpack Accumulation in an Alpine Watershed: A GIS Based Modeling Approach

4.1 Introduction

Winter snow accumulation in alpine watersheds provides most of the streamflow runoff in the western US, Canada and other similar regions in the world (Grant and Kahan, 1974). Under forecast climate warming, winter snow conditions may vary substantially due to macro- and meso-scale climate change. Variations in the relative frequency of dominant synoptic patterns over specific regions in winter result in substantial variability in the winter precipitation over western North America (Changnon et al. 1993; Byrne et al. 1999). Under a climate-warming scenario, dominant patterns may shift northward, resulting in modification of the long-term average precipitation and/or increased inter-annual variability of winter precipitation. Byrne et al. (1999) expects that under climate warming a substantial increase in the frequency of synoptic patterns bringing wet winters to the north western US and southwest Canada and will result in a substantial decline in patterns bringing wet winters to the US southwest.

Leith and Whitfield (1998) studied possible hydrological changes in streams in south-central British Columbia due to forecast climate change. . In the late-fall and early-winter, warmer temperatures would result in more precipitation as rain rather than snow. Due to the fact that a portion of the rainfall would produce runoff, the overall streamflow of this season would increase. These higher late-fall/early-winter streamflows would result in earlier spring runoff and a reduced streamflow in the subsequent summer months (Leith and Whitfield, 1998). However, for all areas, warming will result in an increase in the rain to snow ratio in a watershed. Conversions

likely result in declining runoff, as snowmelt contributes more effectively to river flow than rainfall.

This chapter combines a wide area assessment of forecast changes in wintertime synoptic conditions over western North America (Lapp et al. under review) with a meso-scale alpine hydrometeorology model to evaluate the joint impact(s) of forecast climate change on snowpack conditions in an alpine watershed. The synoptic analysis was used to generate long-term climate time series scenarios using the Canadian Centre for Climate Modeling and Analysis (CCCma) First Generation coupled general circulation model (CGCM1). The alpine hydrometeorology model SIMGRID is used to predict changes in wintertime precipitation at the watershed scale. The SNOPAC model (Sheppard, 1996) is a simple snow routine model that predicts the overall snow accumulation throughout a watershed based on the output from SIMGRID. A vapour transfer model has been incorporated into this SNOPAC model to estimate snow volumes more accurately. The model is applied to a small alpine watershed in the southern Canadian Rockies. The synoptic analysis and GCM output forecasts a modest increase in both winter precipitation and temperatures in the study area. The hypothesis herein, is that the increase in winter precipitation due to synoptic conditions will not compensate for regional changes in the rain to snow ratios. The net result will be a decline in winter accumulations of precipitation as snow, and hence an expected decline in spring runoff.

4.2 Objectives

The key objective is to assess the impact of climate warming on spring snowpack in an alpine watershed in western Canada. To accomplish this the following must be completed:

- develop daily temperature and precipitation scenarios under $1xCO_2$ and $2xCO_2$ conditions,
- adopt a vapour transfer model,
- simulated snow accumulation/ablation for two scenarios for a daily time series of 25 years each (approximately corresponding to 1963-85 and 2021-50),
- compare changes in snowpack for distribution locations and dates for the twenty-five year time periods.

4.3 Study Area

The study area chosen was the upper Oldman River basin in southwestern Alberta (Figure 4.1). The Water Survey of Canada hydrometric gauging station near the intersection of the Oldman River and Highway #22 defines the outlet of this drainage basin. To the west, the basin is bounded by the continental divide separating British Columbia and Alberta. The Whaleback Ridge defines the basin border to the east. The closest climate stations Coleman and Pekisko are located just south and north of the river basin respectively.

The watershed covers an area of 1445 km^2, most of which is covered by alpine boreal forest, (Hungerford et al. 1989). The boreal forest of North America is composed mainly of evergreen conifers such as spruce and fir. The basin contains rugged mountainous terrain with slope angles as high as 68^{o}, and ranges in elevation from 1267 metres at the outlet to 3099 metres at Tornado Mountain. Runoff from this basin flows down the Oldman River through Southern Alberta and into the South Saskatchewan River.

4.4 Alpine Hydro-meteorological Model

The SIMGRID alpine hydrometeorology model (Sheppard, 1996) was set up to operate on the Oldman River Watershed in south-western Alberta. SIMGRID is based on MTCLIM, which uses basic atmospheric physics to forecast temperature, humidity, radiation, and precipitation for outlying areas. MTCLIM was developed by the Intermountain Research Station (Ogden, Utah), as a means of generating climate data for use in fire models, ecological models, insect and disease models, or aiding in the development of silviculture prescriptions (Hungerford et al. 1989) (Figure 4.2). The MTCLIM model predicts daily solar radiation, air temperature, relative humidity, and precipitation for mountainous sites by extrapolating data measured at (BASE) weather stations. In MTCLIM terminology, the location to be simulated is referred to as the SITE and the station for which records exist is known as the BASE. Data is corrected for the differences in elevation, slope, and aspect between the BASE station and the SITE. Data for the BASE weather stations includes daily air temperature, precipitation and dewpoint.

The MTCLIM model predicts a number of variables for one SITE at a time. SIMGRID was developed based on the same input and output variables as MTCLIM but

The Oldman watershed area of 1445 km^2 was subdivided into 100m x 100m pixels. Simulating for all 144, 585 pixels would require hours on a Pentium based personal computer. Classifying the pixels into 120 categories (vs. 144, 558 pixels) reduced the simulation time to minutes. The basin categories were defined in the GIS using attribute ranges as defined in Table 4.1: Ten classes of elevation, three classes of slope, and four classes of aspest. The details of this classification are described in Sheppard (1996). Additional subroutines calculate daily snow accumulation and sublimation for each pixel within the watershed.

4.5 Snow Accumulation/Ablation Model (SNOPAC)

The estimation of snow pack accumulation ant ablation is accomplished through the SNOPAC program, which incorporates an empirically based accumulation model that describes the composition of precipitation based on temperature (Wyman, 1995) and the snowmelt algorithm from the UBC Watershed Model (Pipes and Quick, 1977). Development of the Vapour Transfer Model, which is added to the SNOPAC model, is described below.

The UBC snow melt technique takus into consideration three primary sources of snow melting energy. The first of these, convective heat transfer from warm air, is estimated as being equal to the mean daily temperature above freezing. Second, the net radiant energy gains from shortwave and longwave radiation exchanges is considered. It is represented simply as the daily temperature range. Finally, the latent heat gain from condensation or loss through evaporation at the surface is derived as a function of the range of temperatures. Precipitation was allocated as either liquid (rain) or solid (snow) where mean daily temperature was below freezing. Rain on snow was assumed to freeze

range of temperatures. Precipitation was allocated as either liquid (rain) or solid (snow) where mean daily temperature was below freezing. Rain on snow was assumed to freeze in the snowpack. The snowmelt formulation, adopted from Pipes and Quick (1997), uses daily air temperatures to represent three key energy sources for snow melt.

Daily snow modeling for each pixel was carried out with:

$$SWE_{(t)} = SWE_{(t-1)} + S_{(t)} - Sub_{(t)} - M_{(t)} \qquad (4.1)$$

Where SWE = snow water equivalent (mm)
S = snowfall
Sub = sublimation
M = snowmelt
t = time step in days

4.6 Snow Vapour Transfer Model

This study incorporates a vapour transfer model developed by Thorpe and Mason (1966) and modified by Dery et al. (1998). This model includes four variables that effect vapour transfer: radiation, wind, relative humidity, and air temperature.

Incorporating evaporation/sublimation/condensation into the model requires a vapour pressure difference between the surface and the overlying air, and the transfer rate is dramatically enhanced by wind-generated turbulence. Atmospheric saturation vapor pressures increase with rising temperature while the snow-surface is constrained to the saturation vapour pressure at snow particle temperature. Sublimation occurs when snow-surface vapour pressure exceeds that of the atmospheric vapour pressure and condensation occurs under the opposite conditions. Wind speed is a critical variable; all of the fluxes are directly proportional to wind speed (Leydecker and Melack, 1999).

The change in mass (kg) of a blowing snow particle of radius r (m) due to sublimation per second is given by (Thorpe and Mason, 1966):

$$\frac{dm}{dt} = \left(2\pi r\sigma - \frac{Q_r}{KN_{Nu}T_a}\left[\frac{L_s}{R_v T_a} - 1\right]\right) \Big/ \left(\frac{L_s}{KN_{Nu}T_a}\left[\frac{L_s}{R_v T_a} - 1\right] + R_v \frac{T_a}{N_{Sh} De_i}\right) \qquad (4.2)$$

where:

$2\pi r$ = area function of snow particle (m)

σ = (dimensionless and negative) water vapour pressure deficit with respect to ice ($(e- e_i)/ e_i$), where e and e_i are the actual and saturation vapour pressures at air temperature T_a.

$Q_r = \pi r^2(1- \alpha_p)Q_*$, net radiation transferred to the particle Q_r (W), (Schmidt,1991)

α_p = shortwave particle albedo (0.5) (Schmidt et al. 1998)

Q_* = total incident radiation (W m^{-2})

K = thermal conductivity of air (2.4 x 10^{-2} W m^{-1} K^{-1})

N_{Nu} and N_{Sh} =1.79 + (0.606 $N_{Re}^{0.5}$) (Nusselt and Sherwood numbers)

$N_{Re} = (2rV_r/\upsilon)$ (Reynolds number)

V_r = ventilation velocities (Schmidt, 1982; Dery and Taylor, 1996). Horizontal particle velocity components are assumed equal to the horizontal wind speed

υ = kinematic viscosity of air (1.53x10^{-5} $m^2 s^{-1}$) (Dery and Yau, 1999)

T_a = ambient air temperature (Kelvin)

L_s = latent heat of sublimation (2.838 x 10^6 J kg^{-1})

R_v = gas constant for water vapour (461.5 J kg^{-1} K^{-1})

D = molecular diffusivity of water vapour in air (2.25 x 10^{-5} m^2 s^{-1})

From the rate of mass loss by sublimation (Eqn 2.1) per snow particle we can determine the rate of loss from a unit area by determining the number of particles per unit volume (N(z)). However, the number of snow particles in a cubic metre depends on the particle shape (α) and radius (r_m). In the saltation layer, it is common to assume $\alpha = 5$ and that r_m, the mean particle radius, is 100 μ m (Pomeroy, 1998), although variation in these parameters can be expected with changing environmental conditions. Where $\alpha = 5$, (Dery et al. 1998) the threshold for transport is $N(z) = 9.09 \times 10^7$ m^{-3}.

Hence, by knowing the rate of sublimation per snow particle and the number of particles within a cubic metre of snow we can determine the overall sublimation of a snowpack.

$$Q_{subl} = \frac{dm}{dt} * N(z) \qquad (4.3)$$

where:

Q_{subl} (kg m^{-2} s^{-1}) = total sublimation rate for a column of blowing snow over a unit horizontal land surface,

$\frac{dm}{dt}$ = change in mass (kg) of a blowing snow particle of radius r (m) due to sublimation per second,

$N(z)$ = number of snow particles per unit volume (m^{-3}),

We can calculate the overall sublimation of a snowpack if the approximate number of particles within a cubic metre of the saltation layer are known or estimated as above.

4.7 Methods

4.7.1 Defining daily climate for the study area

Future and Historical temperatures

Historical daily temperatures for the 1xCO2 scenarios were obtained from Environment Canada (1998) for the period of 1962-85. Two BASE stations, Pekisko and Coleman (Figure 4.1) were selected as input climate data stations to predict output for the Oldman River Basin. The $2xCO_2$ temperatures were not as easily obtained. The GCM was used to derive the future temperatures for each of the BASE stations, however, GCM data is given for a 2.5° square and is not considered accurate when looking at areas of

uneven altitude or terrain, such as a mountain area (Clausen and Roth, 1998; Venugopal et al. 1999; Kidson and Thompson, 1998). For these reasons, a direct interpolation from the GCM for temperature data for Pekisko and Coleman for the period of 2021-50 was not considered to be suitable, but the data would be more accurate if a relationship between a prairie location and the two BASE stations could be developed. Lethbridge, Alberta was chosen as the prairie station (located about 150 km south east of the study area). The first step taken was to determine if there was a relationship between the mountain BASE stations and Lethbridge. Daily temperatures for all three stations between 1951-85, (Environment Canada, 1998) were gathered and a linear regression was to compare Lethbridge and Pekisko, and Lethbridge and Coleman. The prediction equations are:

$$T_{Pek} = -2.651 + 0.807\ T_{Leth} \qquad R^2=0.99 \qquad (4.4)$$

$$T_{Col} = -1.229 + 0.791\ T_{Leth} \qquad R^2=0.98 \qquad (4.5)$$

High correlations were found between the prairie station (Lethbridge) and the Pekisko and Coleman stations, with R^2 values of 0.99 and 0.98, respectively. Temperature from the GCM for the $2xCO_2$ period could now be used with more confidence, with the use of Lethbridge temperatures and the regression equations to predict temperatures at Coleman and Pekisko.

Future monthly average temperatures for Lethbridge were taken directly from the CCCma CGCM1 output. Average temperatures for each month of October through March for the period of 2021-50 were derived using ArcInfo. ArcInfo allows the user to specify locations and input mathematical operations. This allowed us to calculate the mean monthly temperatures for each month between the period of 2021-50, for

Lethbridge. These new monthly temperatures were used to predict future Pekisko and Coleman temperatures using regression equations 4.4 and 4.5.

SIMGRID requires daily temperature values. However, the GCM only reports monthly mean air temperatures. The regression equations were used to calculate future monthly mean temperatures for Pekisko and Coleman, based on the Lethbridge mean monthly temperatures. The difference between modeled future monthly average temperatures and observed historical monthly temperatures was calculated, and called temperature change. These monthly temperature changes were converted to daily values, by linear interpolation between the monthly values. Simple linear interpolation proved more effective than a third order polynomial fit - the difficulty in using the polynomial was closing the predictive gap from December 31 to the following January 1. These temperature changes were added to the historical daily data for both Pekisko and Coleman to develop a $2xCO_2$ temperature scenario. This allowed the comparison of the historical snow year of 1962-63 to a future snow year with increased temperatures. The 1962-63 was one of high snow accumulation.

Future precipitation scenarios

Future winter precipitation scenarios were derived using synoptic downscaling data presented in Lapp et al. (under review). Seven key synoptic patterns were adopted that dominate winter precipitation for western North America (Changnon et al. 1993; Figure 4.3). Stepwise multiple linear regression techniques were used to derive relationships between annual historical winter precipitation and the frequency of synoptic patterns for the period 1962-85 for the climate stations at Pekisko and Coleman (Lapp et al. under review).

The following equations represent the linear regression equations for both stations:

$$Pekisko_{ppt} = 9.97\ NWW \qquad R^2 = 0.906 \qquad SE = 70.7\ mm \quad (4.6)$$

$$Coleman_{ppt} = 14.572\ NWW \qquad R^2 = 0.996 \qquad SE = 21.5\ mm \quad (4.7)$$

Note how one dominant pattern influences precipitation at both these locations.

These same seven synoptic pattern frequencies were derived for an approximate $2xCO_2$ scenario (2021-50) to determine the shift or change in pattern frequencies between $1xCO_2$ and $2xCO_2$ (Table 4.3). Daily historical precipitation was simply adjusted using the ratio of the frequency of $2xCO_2$ NWW synoptic patterns to the frequency of historical NWW synoptic patterns to derive a $2xCO_2$ scenario precipitation using the linear regression equations previously determined.

For example, for the Coleman regression, Equation 4.7, NWW is the relative frequency of that pattern in any winter. Hence, for a year where NWW occurs 40% of the time, the winter precipitation for the year would be 583 mm. Under a $2xCO_2$ climate, NWW would increase by 20% of historical values (Table 4.2). Therefore, the precipitation for Coleman is calculated by:

$$Coleman_{ppt} = 14.572 * NWW * (2xCO_2\ NWW / 1xCO_2\ NWW)$$

This same procedure was used to compute the average $2xCO_2$ winter precipitation for the Pekisko climate station.

The change in daily average temperatures and precipitation between the period 1962-85 and 2021-50 is shown in Figure 4.4, for both stations. The figure clearly shows the greater winter warming trend of approximately 4°C; and a lesser warming of approximately 1-2°C in early fall and spring.

The temperature and precipitation scenarios were applied to the Oldman River Basin with the SIMGRID and modified SNOPAC models to evaluate the net change in maximum winter snowpack for the period 1962-85, and 2021-50.

4.8 Sensitivity Analysis of the Sublimation Model

The sublimation model adopted from Dery et al. (1998), consists of four environmental inputs: Incident solar radiation, R (W/m^2); Wind velocity, V (m/s); Ambient air temperature, T_a (K) (assumed to be average daily temperature); and Relative Humidity, RH (%). Figure 4.5 shows how each variable affects the rate of sublimation, assuming all other variables are held constant at mean values. For example to determine how sensitive sublimation is to wind, radiation, relative humidity and air temperature were all held constant while changing the value of wind speed over an expected range. Relative humidity was held at 50%, air temperature at 2°C, radiation at 1800 kJ/m^2, and wind speed at 0 m/s throughout the sensitivity analysis.

According to this sensitivity model sublimation is most affected by wind speed. For speeds up to 12 m/s, sublimation rates can be as high as 200 mm/winter SWE (Figure 4.5). Radiation is also a major influence on the amount of sublimation over the 180 days, with amounts also nearing 200 mm/winter. Temperatures reaching 15°C can increase sublimation to about 90 mm/winter. Sublimation was around 60 mm/year when relative humidity was its lowest values of 0%, which rarely ever occurs.

Based on this sensitivity analysis the greatest interested will be in the effects that wind and radiation play in the role of vapour transfer to and from the snowpack.

4.9 SNOPAC: Over-Winter Model

The key innovation herein is the addition of a vapour transfer model to the over-winter snow model. Hence the key question is: Does this vapour transfer model increase the accuracy of the SNOPAC model? It is a well-known fact that sublimation and condensation occur within a snowpack, and the vapour transfer model is, therefore, expected to improve the accuracy of the snow model.

Southern Alberta is quite famous for chinooks and many sunny winter days. Wind and radiation are the variables most affecting over-winter sublimation. Daily values of relative humidity, air temperature, and incident solar radiation are simulated with SIMGRID. Wind data for the validation runs was used from the years 1984 and 1989 from the Akamina, AB station (K. Runions, Alberta Environment, personal communication 2001). Daily wind data used for the snow pack analysis was obtained for Lethbridge during the period of 1998-2000 (L. Flanagan, University of Lethbridge, personal communication, 2001).

Monthly snow pillow data was only available for the years of 1984 and 1989 for Race Horse Creek and Lost Creek, snowpillows located within and near the Oldman River Basin (Figure 4.1). These monthly snowpillow data values were interpolated into daily values through linear interpolation. Wind data was not available for Race Horse Creek for 1989; hence no comparison was carried out.

Figure 4.6 compares the snow pillow data to that the SNOPAC model (without vapour transfer model) and SNOPAC-VAP (with vapour transfer model). The key interest in this study is snow accumulation over the winter season, up to April 1st, thus no melting is considered. It is to be noted how the SNOPAC-VAP model shows slightly

better accuracy in predicting snowpack depths compared to the snowpillow data. In all three comparisons the SNOPAC-VAP model gives snow estimates more similar to the snow pillow data in the both the early season and late season, towards April 1, than does SNOPAC.

The meaningful snowpillow data consisted of only twelve points – four single monthly values for 1984 and 1989 at Racehorse Creek, and four points for 1984 at Lost Creek. Hence, the SNOPAC and SNOPAC-VAP models estimated on those days were compared to the actual snowpillow observations on those dates (Table 4.3). Therefore, the regression comparison, based on n=12, is limited in use. Nevertheless, more data was not available.

The modeled snowpack values were taken from both models and compared directly to those of the snowpillow values, through simple linear regression (Table 4.4). Comparing R^2 and standard error show virtually no difference between the two models results. However it is important to note the difference between the slopes and constant of each regression equation. In a perfect regression analysis $y = ax + b$, one would expect a=1.0 (slope) and b=0 (constant) for the line of best fit. Following these results we see using the SNOPAC-VAP model, the slope is 0.938 is closer to one, compared to SNOPAC, which has a slope of 0.893. The regression constant of 8.021 for the SNOPAC-VAP model also shows an overall improvement compared to that of SNOPAC with an intercept value of 15.613. A negative constant is hard to justify, as it is impossible to have a negative snowpack value. The SNOPAC-VAP model shows a modest improvement in predicting snow accumulation compared to the SNOPAC model.

4.10 Results and Discussion

The SWE model suggests a general trend of declining snowpack in winter under global warming. The result follows the original hypothesis: the increase in temperature results in a conversion of much of the winter precipitation to rainfall: and hence snowpacks decline quite radically. The following discussion highlights the key points.

A comparison between 2 different pixel categories (classes defined by the GIS as in Table 4.1) illustrates the overall difference. Consider two snow zones in the watershed: category 14 (elevation 1401-1600m, slope 0-42%, aspect east) and category 50 (elevation 2001-2200m, same slope and aspect). These categories (east facing slopes) receive less energy than west slopes; hence snowpacks last longer into the spring. Time series analyses of precipitation and snowpack accumulation over the 1973-74 winter are presented in Figure 4.7 (categories 14) and Figure 4.8 (category 50). The 1973-74 snow year was one of high snowpack accumulation.

Figure 4.7 shows the comparison between $1xCO_2$ and $2xCO_2$ wintertime precipitation and snow accumulation for Category 14 using the SNOPAC-VAP model. Observations include:

- The cumulative precipitation over-winter is clearly higher for the $2xCO_2$ scenario,
- There is dramatic decline in snow accumulation for a $2xCO_2$ winter, the snowpack declines to zero six times over-winter,

Figure 4.8 shows the relationship between wintertime precipitation and snow accumulation for Category 50 under a $1xCO_2$ and a $2xCO_2$ scenario using the SNOPAC-VAP model. Observations include:

- The cumulative precipitation over-winter is again clearly higher for the $2xCO_2$ scenario,

- Substantially colder conditions over-winter at higher elevation result in a snowpack that does not melt out as dramatically as lower elevations. But even above 2000m, there are still several melting phases that occur over-winter in a $2xCO_2$ environment,

Figures 4.7 and 4.8 show there will likely be moderate losses in upper elevation snowpacks and significant losses in low elevation snowpacks, resulting in a substantial decline in overall basin spring snow equivalent.

The average trend over the twenty-four years of study for the two categories is shown in Figure 4.9 (Category 14) and 4.10 (Category 50). Historical trends show a steady increase in snowpack over-winter for the entire watershed, as indicated by the blue shaded bars in both Figures 4.9 and 4.10. The red bars represent $2xCO_2$ conditions; these show very similar results to the historical conditions, however with a smaller magnitude. Equally important, the $2xCO_2$ snowpack never accumulate as much SWE at any time during the winter period as the historical conditions. For example, on February 1st, the average $2xCO_2$ SWE is less than half of the average value under historical conditions. The overall importance of these figures is to note the temporal change in snowmelt out at lower elevations – this occurs much earlier under $2xCO_2$ conditions.

The spatial distribution of snowpack for the watershed for April 1, 1974 $1xCO_2$ and $2xCO_2$ climate, and for March15, 1974 $2xCO_2$ conditions in shown in Figures 4.11,4.12 and 4.13 respectively. These two dates were chosen as near peak snow accumulation dates for the two climate scenarios. Figure 4.12 (historical) clearly shows a substantially greater expanse of snow cover at low and medium elevations. Only at very high elevations has $2xCO_2$ snowpack accumulation remained anywhere near historical values. Overall the snowpack in a warmer climate has decreased to nearly 50% of historical accumulations. It is obvious from this comparison that temperature plays a key

role in the accumulation of snowpack, as temperatures are typically colder at higher elevations.

4.11 Basin Runoff Potential

Throughout the entire basin the annual total volume of change in SWE (m^3) for the $2xCO_2$ and $1xCO_2$ scenarios for maximum snowpack values were calculated. The basin snow water equivalent on the date of maximum snowpack accumulation was used as an indicator of runoff potential under climate warming (Table 4.5). Areas were calculated for each category and maximum snowpack values for each category were summed over the entire basin to determine the snow water equivalence for available snowpack runoff in cubic metres. Extreme snow accumulation may occur when temperatures stay moderately cold even under climate warming conditions. Table 4.5, shows how maximum SWE over the watershed can fluctuate annually based on temperatures and precipitation. In 1963 the $2xCO_2$ SWE increases substantially over the historical SWE, which could result in possible spring flooding. However, this is the only year out of 22 years when this occurred. A flooding potential does exists under the right conditions of a cold winter with increased precipitation.

The average basin volume over the historical period is nearly fifty percent greater than that for $2xCO_2$ conditions (Table 4.5). The trend under 2xCO2 condition is that the average SWE for the basin declined. Hence, in most years, the water supply will decline; but in a few cold years the snowpack may be much greater, enhancing flooding potential

4.12 Summary

A snow modeling routine has been adapted to model snowpack accumulation and ablation over-winter in an alpine environment. GCM forecasts of future temperature and precipitation developed through the CGCM1 were used to create $1xCO_2$ and $2xCO_2$ climate scenarios for a twenty-two year daily climate database for the Upper Oldman River watershed, Southern Alberta, Canada.

Modeling of snow accumulation and ablation under both scenarios indicates climate warming will result in a substantial decline in the over-winter snow accumulation in the watershed in most years.

The modeling results herein reveal that annual runoff volumes may substantially decrease with the decline in snowpacks, and that runoff that does occur would likely be modest events due to midwinter melting of lower elevation snow. However, the data also support the contention that cool winters may coincide with dramatic precipitation, resulting in larger snow accumulations that could lead to increased flood potential.

Overall, the prospect of a decline in available annual streamflow would place substantial stress on much of western Canada. The stress would be particularly severe for those regions with substantial development based on a more abundant water supply. The irrigation industry, as the greatest single consumer of water in the region, will likely come under the greatest scrutiny and stress.

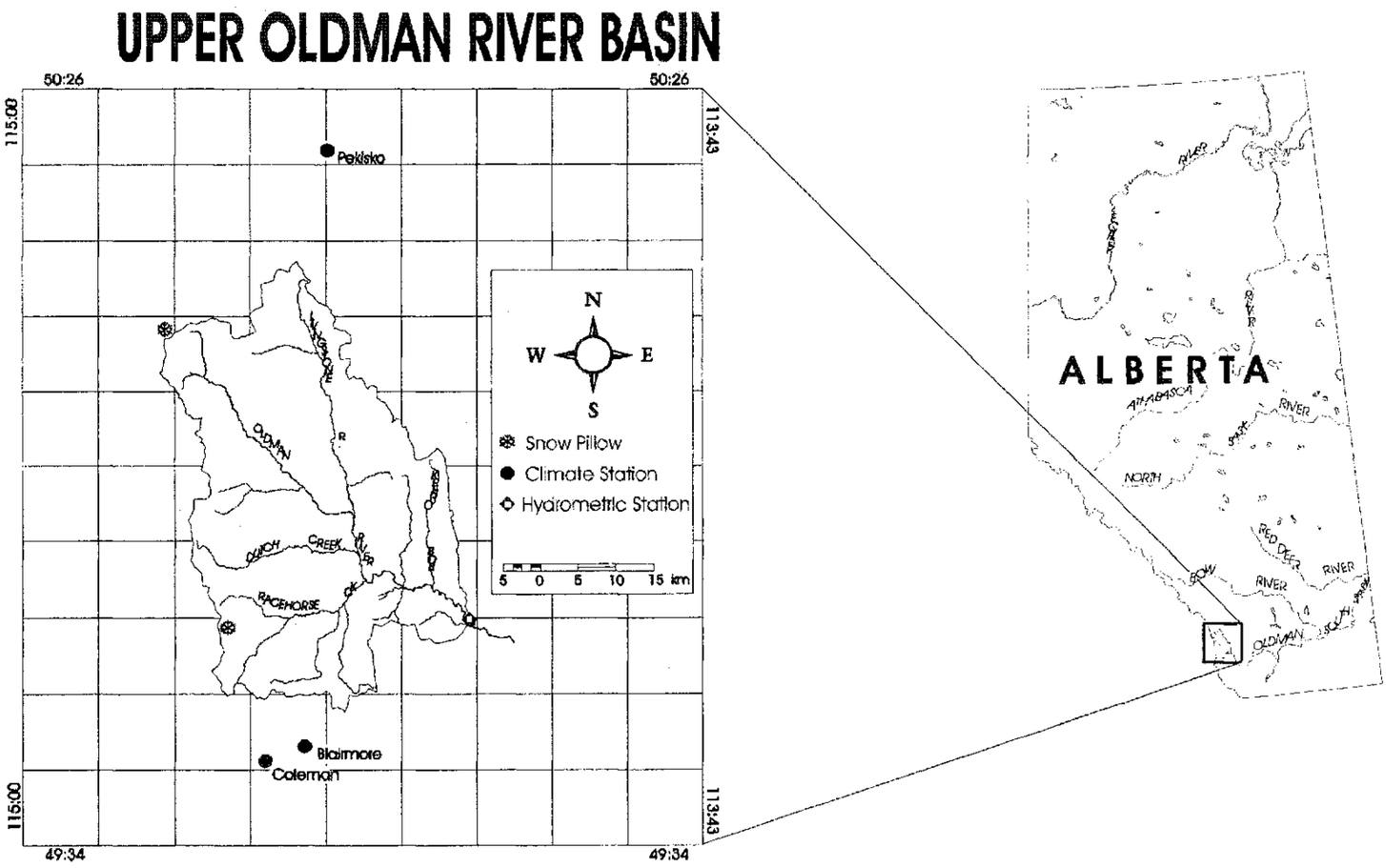

Figure 4.1 Location of the Upper Oldman watershed in southwestern Alberta, Canada (Sheppard 1996).

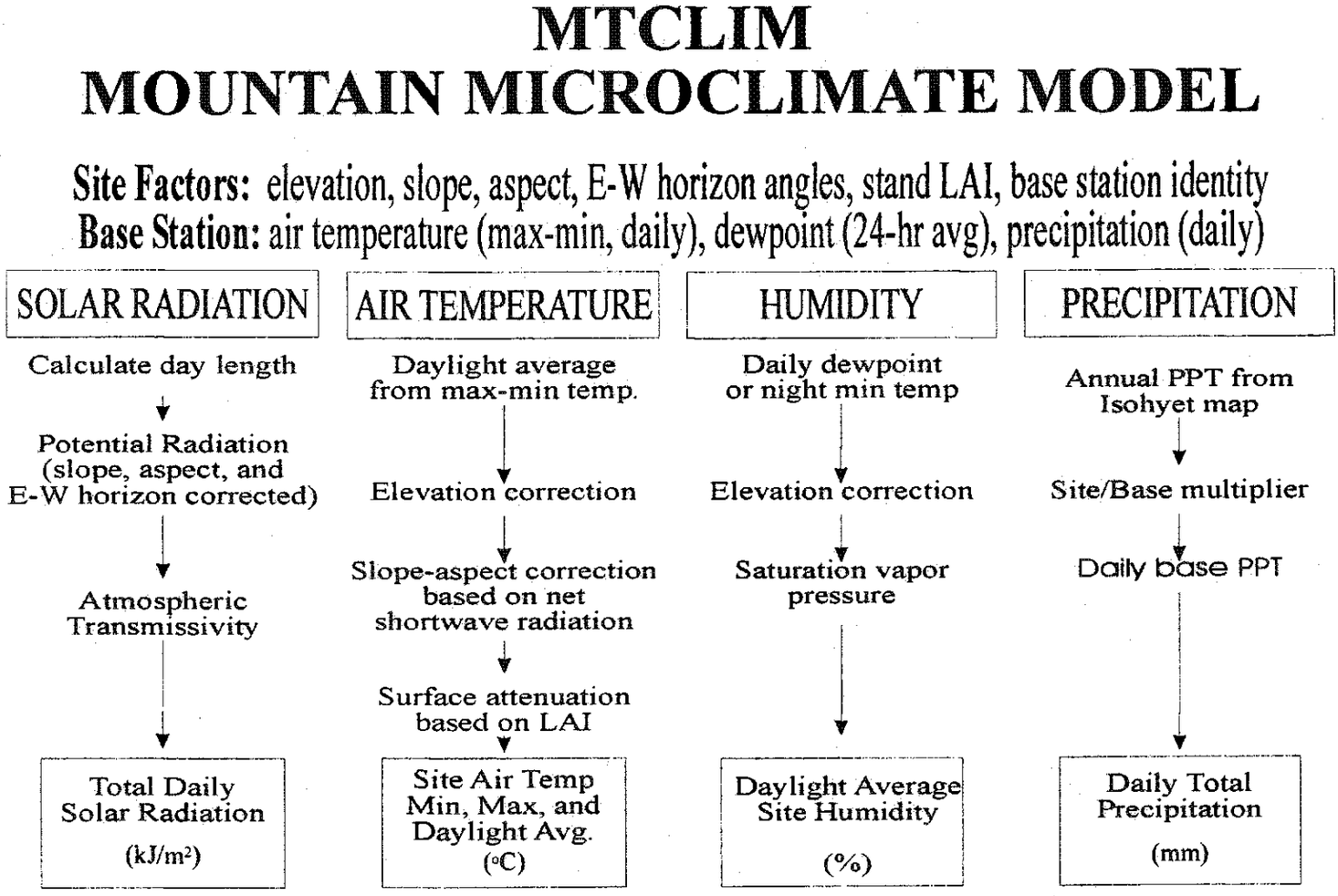

Figure 4.2 Flowchart of the MTCLIM model (after Hungerford et al. 1989).

Table 4.1 Slope, elevation and aspect attributes used to define the 120 categories from 144,558 pixels in the Upper Oldman watershed.

Slope (%)	% of basin area
0 - 42	74.94
43 - 102	23.93
103 - 250	1.13
Elevation (m)	
1200 - 1400	2.75
1401 - 1600	14.21
1601 - 1800	26.03
1801 - 2000	28.82
2001 - 2200	19.04
2201 - 2400	7.02
2401 - 2600	1.72
2601 - 2800	0.36
2801 - 3000	0.05
3001 - 3200	0.003
Aspect	
North	20.00
South	21.00
West	25.00
East	34.00

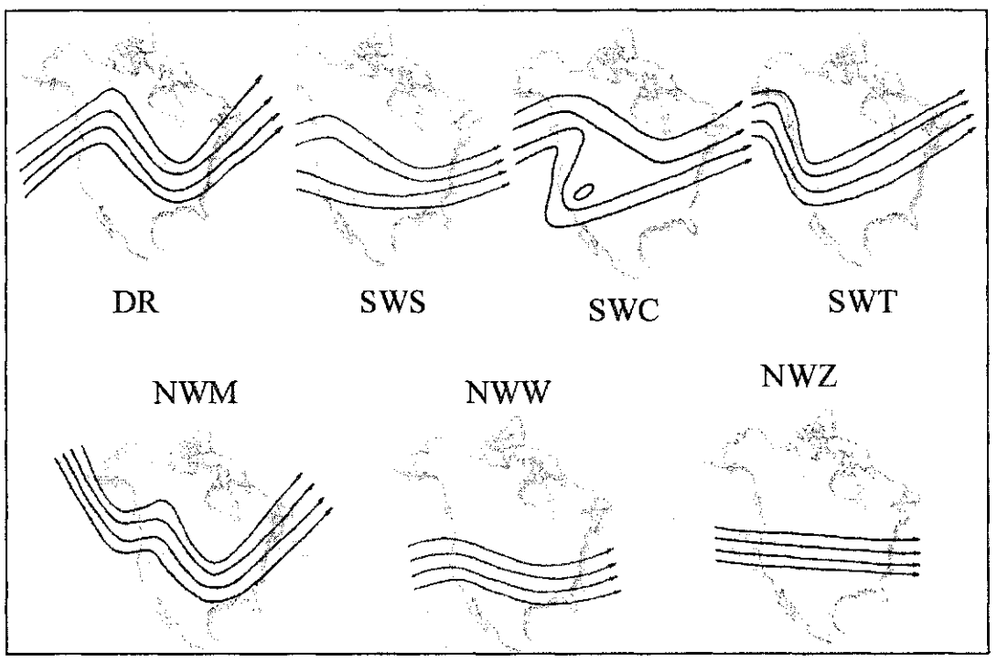

Figure 4.3 The seven dominant synoptic 50-kPa patterns as defined by Changnon et al. (1993). The ridge pattern (DR) is associated with dry anomalies over the entire region. The split-flow pattern (SWS) is associated with wet anomalies across southern regions. The cutoff pattern (SWC) is associated with wet anomalies across southern regions. The trough pattern (SWT) is associated with wet anomalies across southern regions. The meridional northwest pattern (NWM) is associated with wet anomalies across northern regions. The west-northwest pattern (NWW) is associated with wet anomalies across northern regions. The zonal pattern (NWZ) is associated with wet anomalies across northern regions.

Table 4.2 Average Annual Frequency for the Historical and 2 xCO_2 50-kPa Synoptic Patterns (* Historical Frequencies for the period of 1951-85).

	DR	NWM	NWW	NWZ	SWT	SWS	SWC
Changnon	10.7	15.2	21.9	3.3	25.5	4.5	16.6
$1xCO_2$	13.2	15.1	18.6	4.0	26.0	4.2	16.7
$2xCO_2$	23.7	15.0	26.4	4.6	19.2	3.9	6.3

*Frequency is given in percent. Annual values do not add up to 100% due to unclassified days.

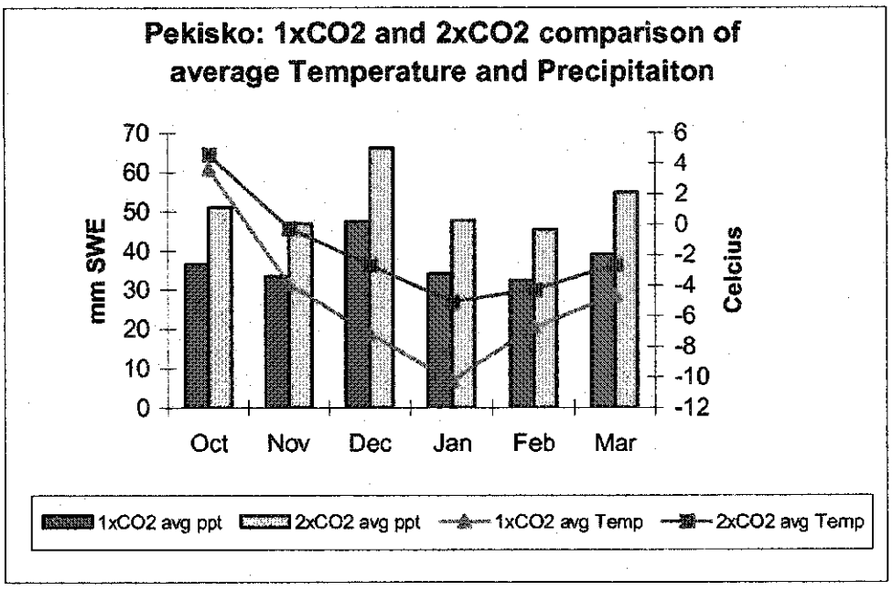

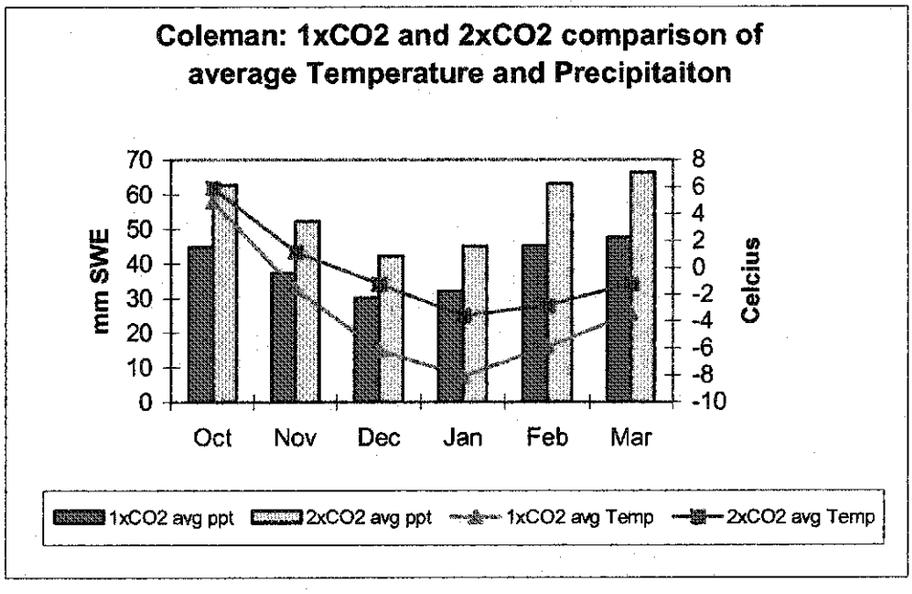

Figure 4.4 $1xCO_2$ and $2xCO_2$ average change in precipitation and temperature over the winter, October through March, for Pekisko and Coleman.

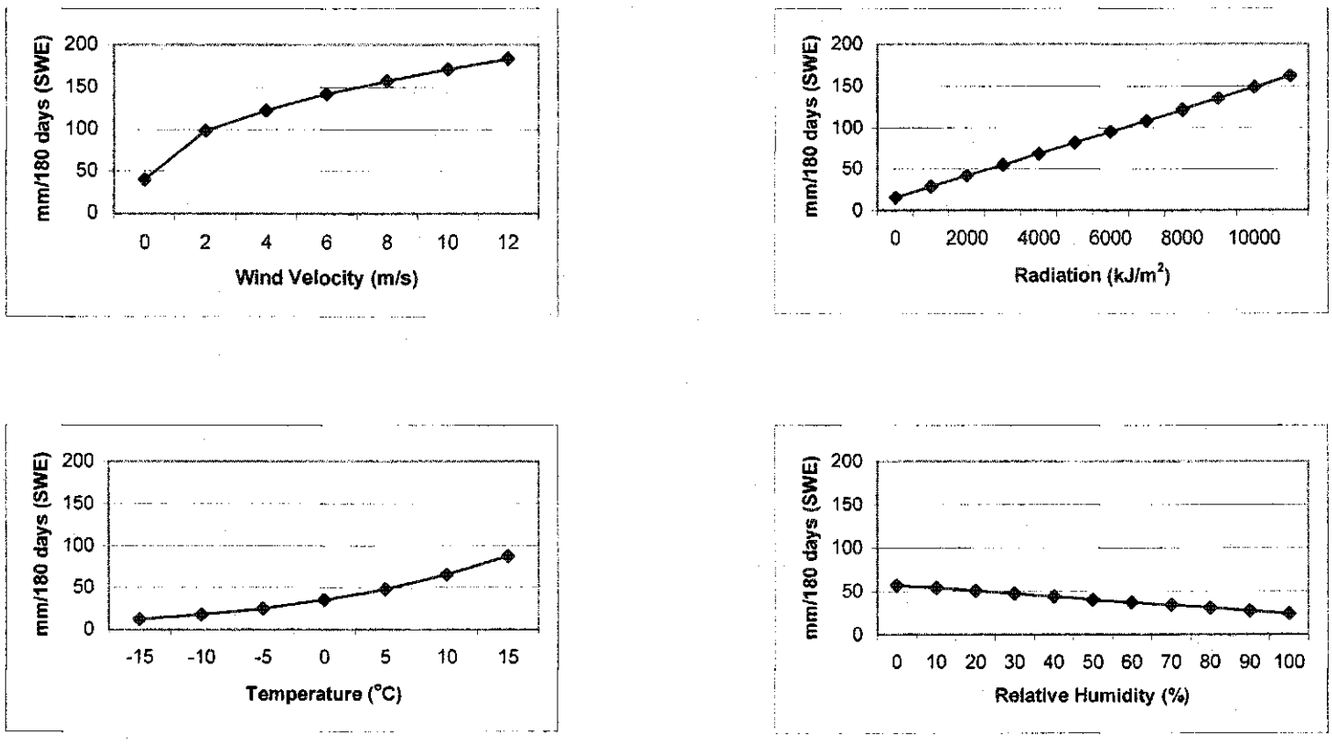

Figure 4.5 Sensitivity Analysis for the sublimation model, comparing wind velocity, radiation, temperature, and relative humidity, based over 6 months (Oct 1- Mar 31).

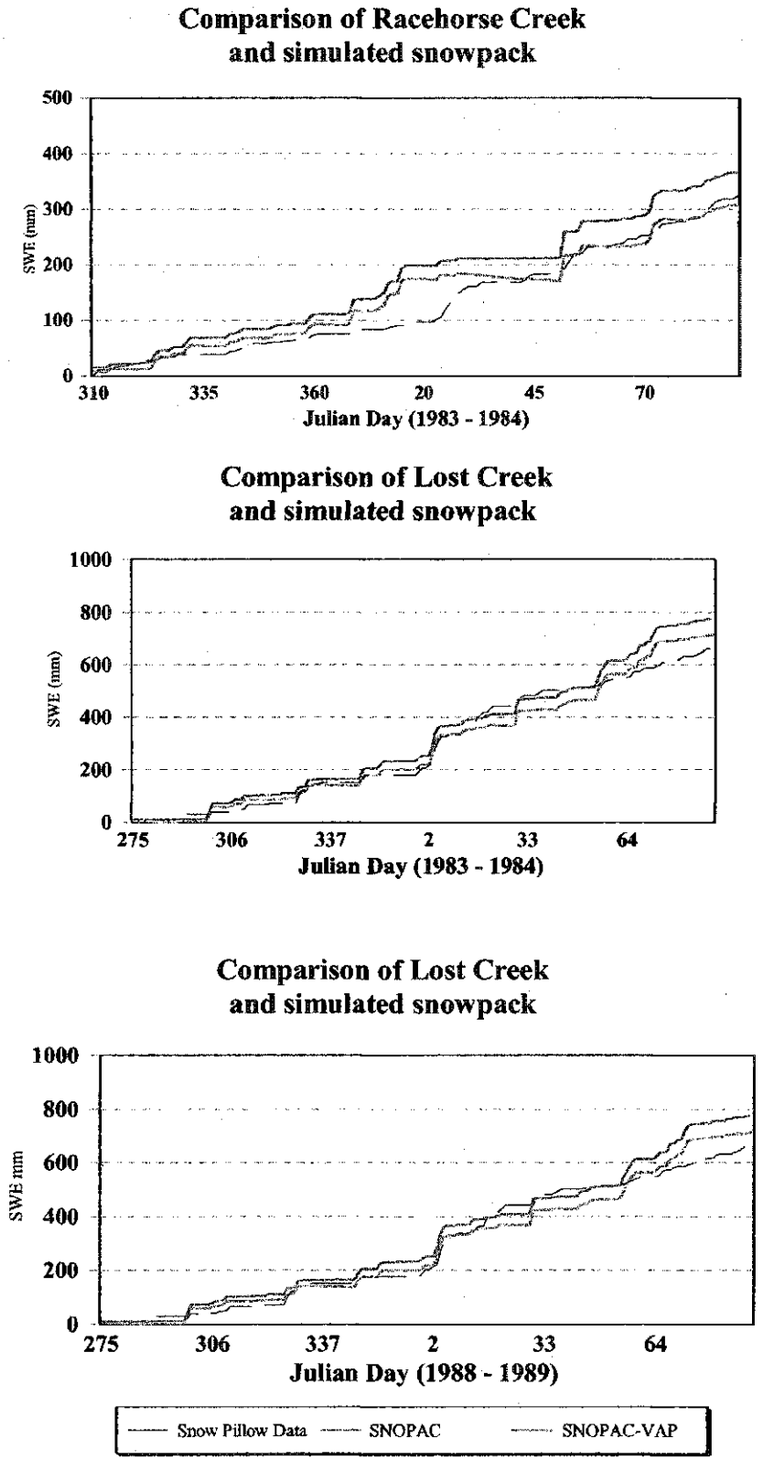

Figure 4.6 Comparing SNOPAC and SNOPAC-VAP snow models to smoothed snowpillow data at Lost Creek and Racehorse Creek. 1983-84; 1988-89.

Table 4.3 Comparing recorded SWE (mm) snowpillow data to the SNOPAC and SNOPAC-VAP models at Lost Creek and Racehorse Creek. Four single monthly values for 1984 and 1989 at Racehorse Creek, and four points for 1984 at Lost Creek. (n=12)

		Lost Creek			Racehorse Creek		
	Jday	Snow Pillow	SNOPAC	SNOPAC-VAP	Snow Pillow	SNOPAC	SNOPAC-VAP
1984-85	32	193	270.7	240.9	188	212.2	182.3
	59	272	354.5	311.2	254	279.3	234.1
	87	328	453.1	400.2	320	358.8	301.9
1988-89	1	205	252.8	219.6			
	32	482	469.3	425.7			
	61	549	614.8	563.7			
	91	661	776.4	714.3			

Table 4.4 Simple linear regressions calculated between the snow pillow data and those of the corresponding snow pack on that date modeled with SNOPAC and SNOPAC-VAP.

Model	R^2	St. Error	Constant	Slope
SNOPAC	0.945	40.6	-15.613	0.893
SNOPAC-VAP	0.945	40.7	8.021	0.938

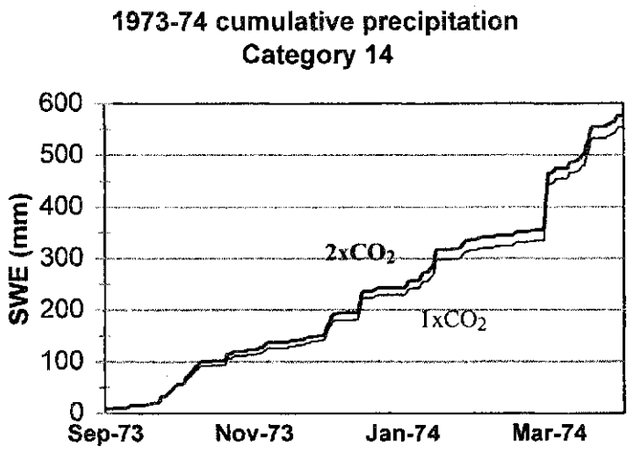

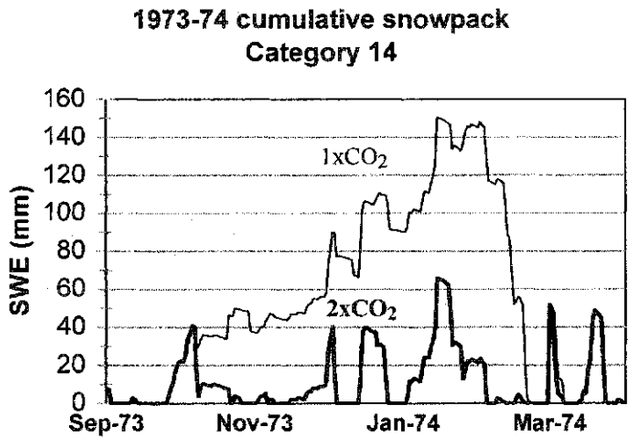

Figure 4.7 Time series of (a) cumulative precipitation for the winter period for category 14 (elevation 1401-1600m, slope 0-42%, aspect east) under $1xCO_2$ and $2xCO_2$ conditions; and (b) snowpack for the same period and conditions. Note the y-axis scale change.

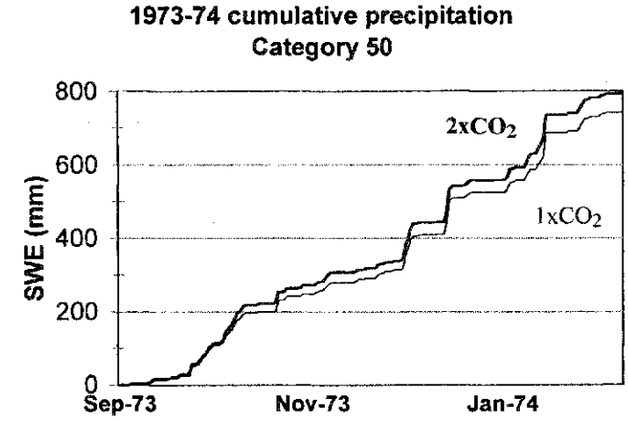

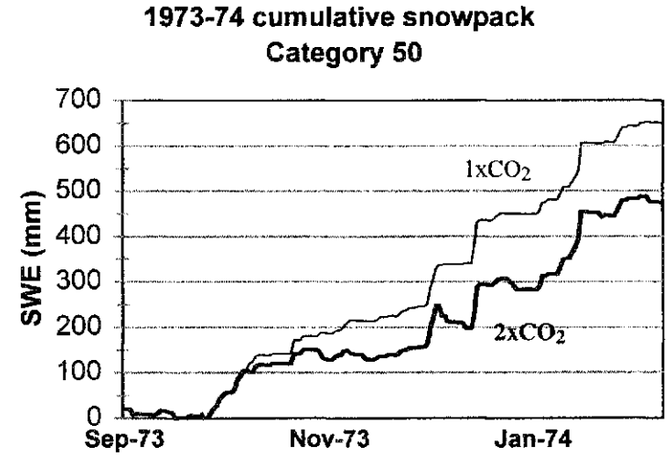

Figure 4.8 Time series of (a) cumulative precipitation for the winter period for category 50 (elevation 2001-2200m, slope 0-42%, aspect east) under $1xCO_2$ and $2xCO_2$ conditions; and (b) snowpack for the same period and conditions. Note the y-axis scale change.

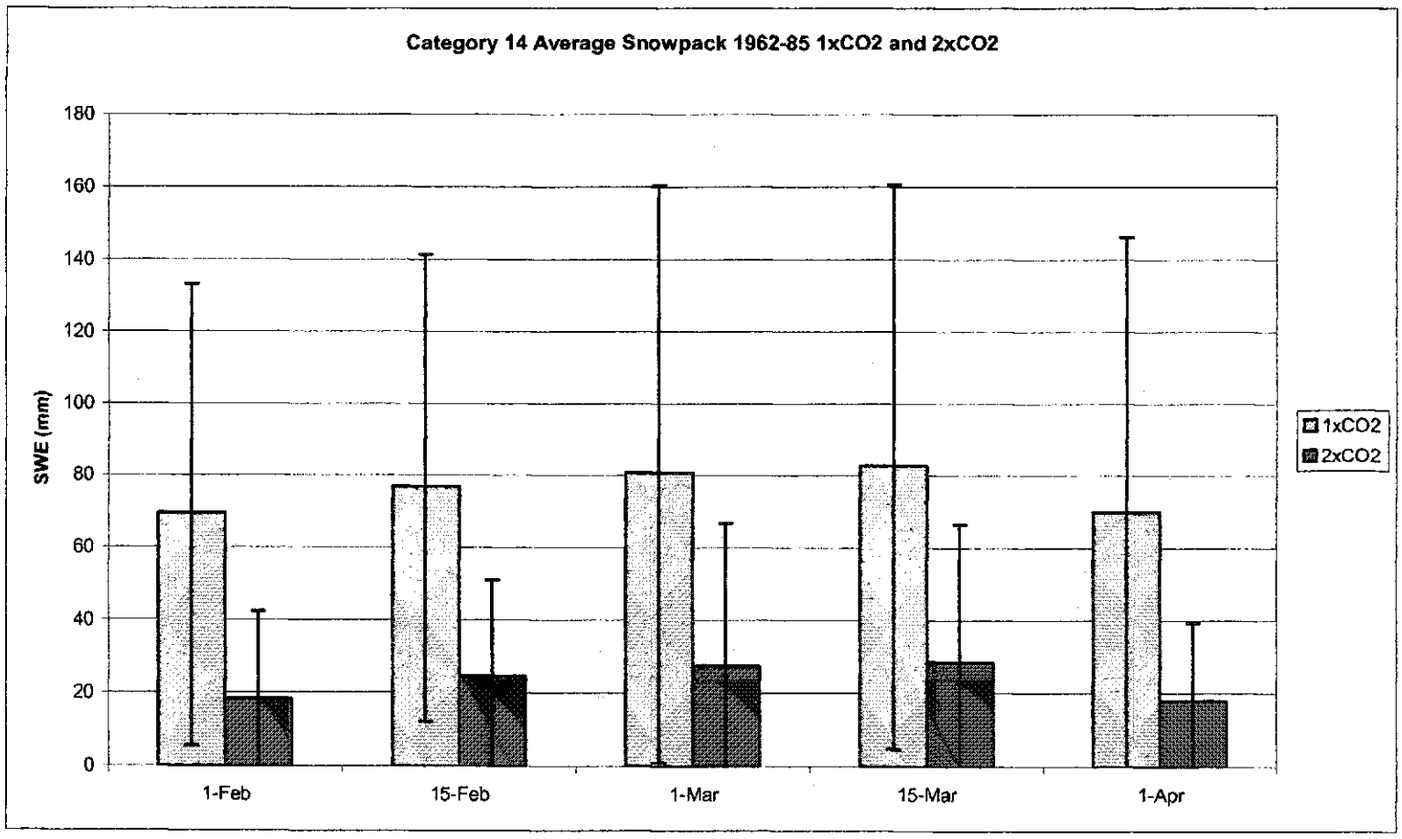

Figure 4.9 Time series of average SWE over category 14 as simulated with SIMGRID for the $1xCO_2$ and $2xCO_2$ winter climate scenarios. Error bars represent standard deviation.

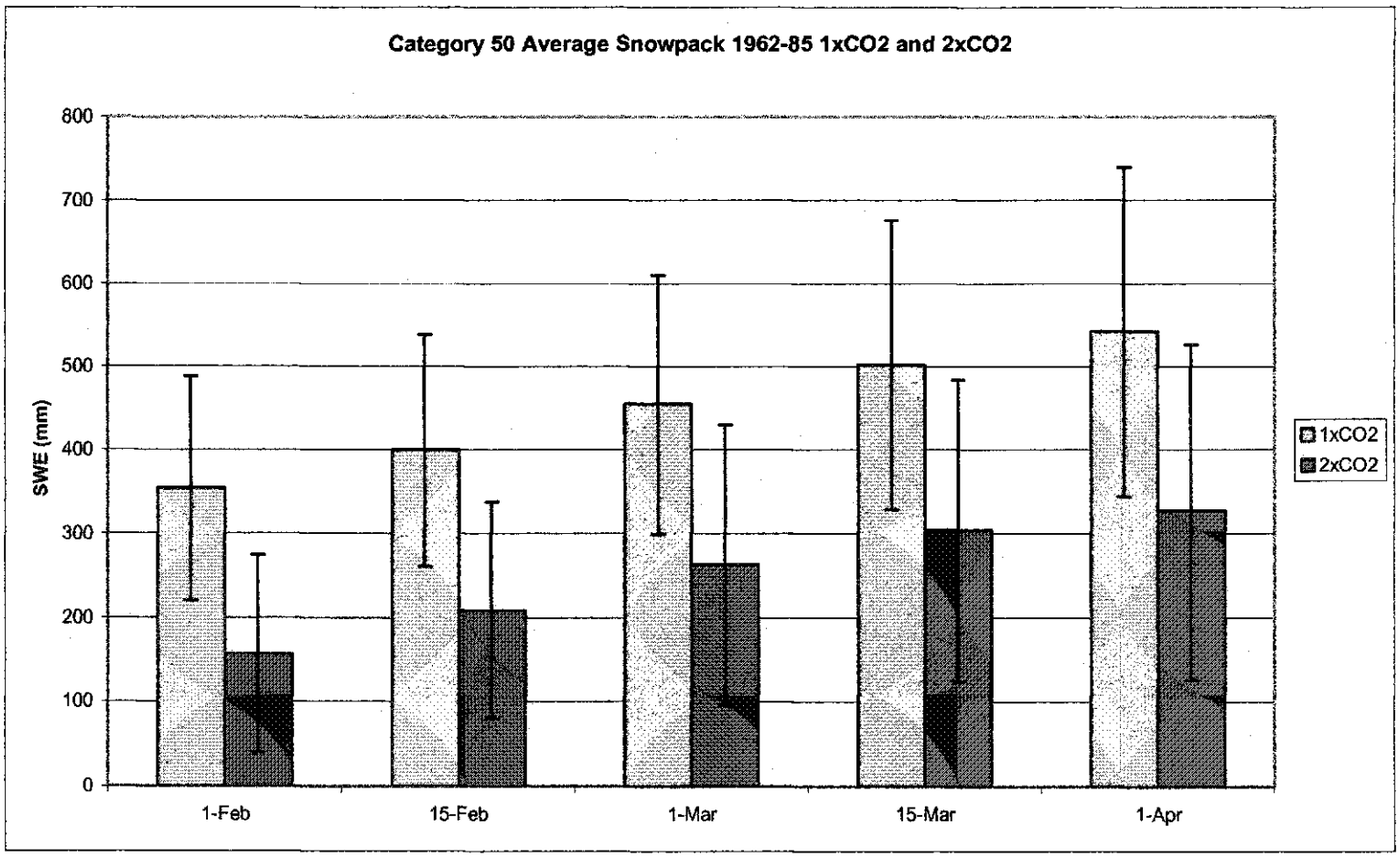

Figure 4.10 Time series of average SWE over category 50 as simulated with SIMGRID for the $1xCO_2$ and $2xCO_2$ winter climate scenarios. Error bars represent standard deviation.

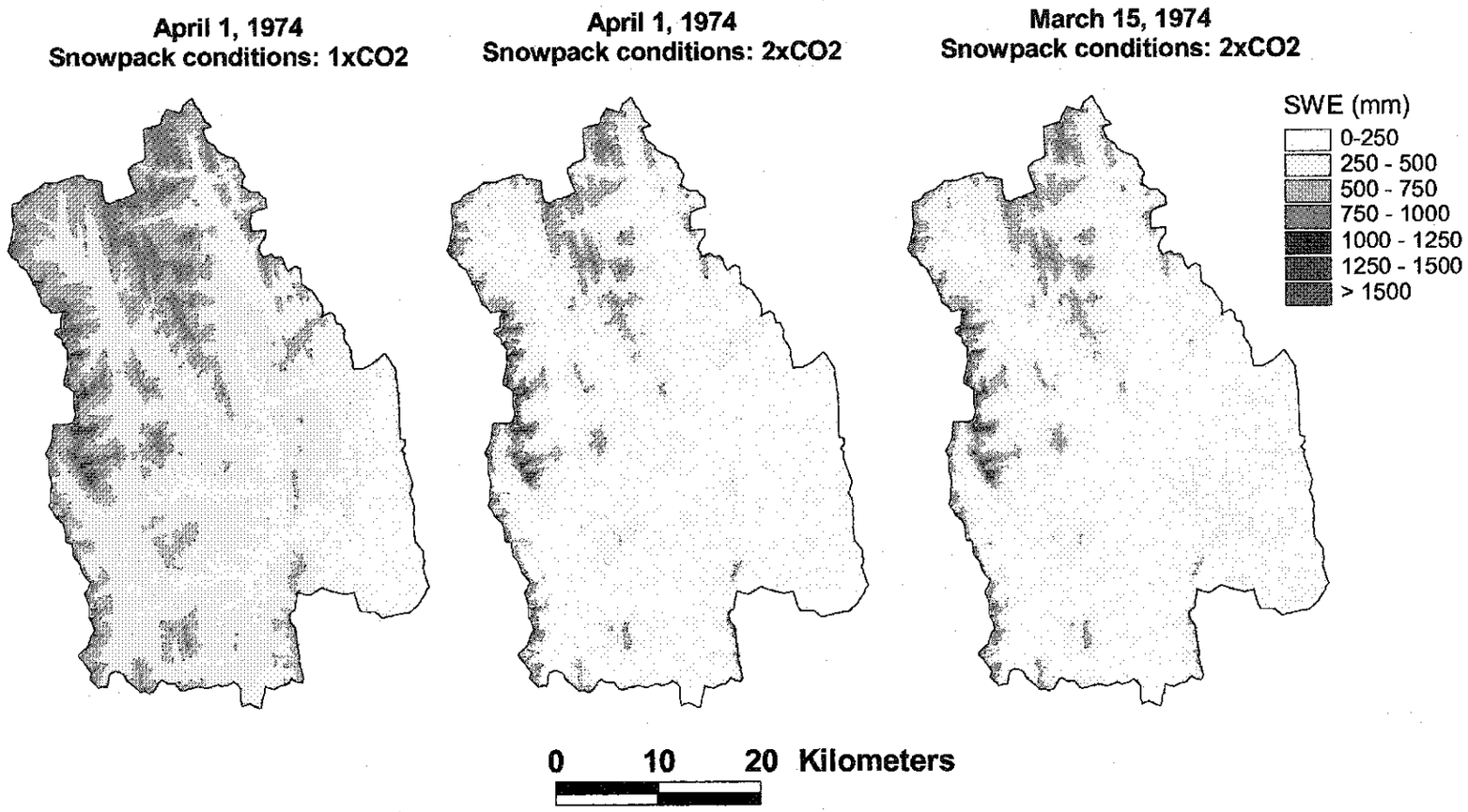

Figure 4.11 SWE (mm) over the watershed on April 1, 1974. Historical conditions.

Figure 4.12 SWE (mm) over the watershed on April 1, 1974. $2xCO_2$ conditions.

Figure 4.13 SWE (mm) over the watershed on March 15, 1974. $2xCO_2$ conditions.

Table 4.5 Differences in SWE volume (million m^3) over the entire Oldman River Basin between historical and $2xCO_2$ conditions.

	$1xCO_2$	$2xCO_2$
1963	305	**328**
1964	572	333
1965	664	330
1966	459	319
1967	965	546
1969	780	632
1970	706	507
1971	922	434
1972	1266	874
1973	446	189
1974	775	498
1975	832	647
1976	468	204
1977	276	128
1978	571	324
1979	719	538
1980	581	256
1981	419	289
1982	620	425
1984	403	137
1985	523	269
mean	632	391
st. dev	238	187

Chapter 5
Summary and Recommendations

5.1 Summary

This study has adapted GCM synoptic downscaling analysis to develop winter precipitation scenarios for selected climate stations in western North America. The spatial characteristics of the CCCma CGCM1 50-kPa were visualized within a GIS, and circulation patterns were visually classified into one of seven mutually exclusive 50-kPa wintertime synoptic patterns described by Changnon et al. (1993).

The first step to determine whether the GCM was accurately displaying climate warming was to validate the model with historic pattern frequencies. The simulated $1xCO_2$ synoptic frequencies were compared to historical data, and the GCM model was found to be robust. Reliability could now be employed in the model for the forecasting of $2xCO_2$ scenarios. Pattern frequencies from $2xCO_2$ were compared to historic frequencies to determine which patterns were predicted to exhibit significant differences under a climate-warming scenario. An interpretation of these differences in synoptic flows points to considerably wetter conditions in the northern United States and southern Canada on the west coast to Northern California. Considerably dryer conditions are forecast in the central and southern Rocky Mountain States (Figure 3.2).

A micrometeorology model has been applied to model snowpack accumulation and ablation over-winter in an alpine environment. GCM forecasts of future temperature and precipitation developed through the CGCM1 were used to create $1xCO_2$ and $2xCO_2$ climate scenarios for a twenty-two year daily climate database for the Upper Oldman River watershed, southern Alberta, Canada.

Modeling of snow accumulation and ablation under both scenarios indicates climate warming will result in a substantial decline in the over-winter snow accumulation of up to 30% throughout the watershed in most years.

The modeling results argue that annual runoff volumes may substantially decrease with the decline in snowpacks, and that runoff that does occur would likely be modest events due to midwinter melting of lower elevation snow. However, the data also support the contention that cool winters may coincide with dramatic precipitation, increasing snow accumulations and possible flooding threat.

5.2 Recommendations

The next step in this research is to determine the extent to which runoff is affected by climate warming. Even though this research has predicted that snowpacks could decline as much as 50% under 2xCO2 conditions, will runoff also decrease by 50% or will there be even a greater impact on runoff as the overall soil and vegetation structure could change. What type of an effect will these changes result in for humans who depend upon runoff from our river systems?

A better understanding of winter climate variability, therefore, can affect policy decisions concerning water releases from dams, aid in anticipating water shortages, and identify likely locations of high snowfall amounts. These assessments can then be used as valuable information for policy makers and managers as well as forecasting tools for future climatic events.

5.0 References

Ayers, M.A., D.M. Wolock, G.J. McCabe, and L.E. Hay. 1990. Simulated hydrological effects of climatic change in the Delaware River basin, paper presented at the joint meeting of the American and Canadian Water Resources Associated, Toronto, Ont., Canada, April, 1990.

Balling, R.C. Jr., P.J. Michaels, and P.C. Knappenberger. 1998. Analysis of winter and Summer Warming Rates in Gridded Temperature Time Series. Climate Research **9,** 175-181.

Boer, G.J., Flato, G., Reader, M.C., Ramsden, D. 2000. A transient climate change simulation with greenhouse gas and aerosol forcing: experimental design and comparison with the instrumental record for the twentieth century. Climate Dynamics **16,** 405-425.

Boer, G.J., N.A. McFarlane, and M. Lazare. 1992. Greenhouse Gas-induced Climate Change Simulated with the CCC Second-Generation General Circulation Model. J. Climate **5**, 1045-1077.

Bohr, G.S. and E. Aguado. 2001. Use of April 1 SWE measurements as estimates of peak seasonal Snowpack and total cold-season precipitation. Water Resources Research **37,** 51-60.

Busuioc, A., von Storch, H. and Schnur, R. 1999. Verification of GCM generated regional precipitation and of statistical downscaling estimates. Journal of Climate **12,** 258-272.

Byrne, J.M., Berg, A., Townshend, I. 1999.Linking observed and general circulation model upper air circulation patterns to current and future snow runoff for the Rocky Mountains. Water Resources Research **35,** 3793-3802.

Cain, N. 1975. An elevational control of peak Snowpack variability. Water Resources Bulletin **11,** 613-621.

Canadian Centre for Climate Modelling and Analysis. http://www.cccma.bc.ec.gc.ca. 2000.

Carleton, A.M., D.A. Carpenter, and P.J. Weser. 1990. Mechanisms of Interannual Variability of the Southwest United States Summer Rainfall Maximum. Journal of Climate **3,** 999-1015.

Cavazos, T. 1997. Downscaling Large-scale Circulation to Local Winter Rainfall in North-eastern Mexico. International Journal of Climatology **17**, 1069-1082.

Cayan, D. 1996.Interannual climate variability and snowpack in the western United States, Journal of Climate **9,** 928-948.

Changnon, D., McKee, T.B. and Doesken, N.J. 1993. Annual snowpack patterns across the Rockies: long-term trends and associated 500-mb synoptic patterns. Monthly Weather Review **121**, 633-647.

Changnon, D., T.B. McKee, and N.J. Doesken. 1991. Hydroclimatic variability in the Rocky Mountains, Water Resources Bulletin **27,** 733-745.

Clausen, A. and R. Roth. 1998. Statistical downscaling of subgridscale precipitation. IAHS-AISH **254,** 79-85.

Conway, D., Wilby, R.L. and Jones, P.D. 1996 Precipitation and air flow indices over the British Isles. Climate Research **7,** 169-183.

DeMaria, M., and R. E. Tuleya, 2000. Evaluation of quantitative precipitation forecasts from the GFDL Hurricane Model. In Symposium on Precipitation Extremes ,Boston, MA: American Meteorological Society 340-343.

Dery, S.J., Taylor, P., and J. Xiao. 1998. The thermodynamic effects of sublimating, blowing snow in the atmospheric boundary layer. Boundary-Layer Meteorology **89,** 251-283.

Dyunin,A. K.; Kvon, Ya,D., Zhilin,A.M. and A.A. Komarov. 1991. Effect of snow drifting on large-scale aridization. Glaciers-ocean-atmosphere interactions. Proc. symposium, St. Petersburg, 1990. (IAHS; Publication) **208,** 489-494.

Easterling, W.E. 1997. Why Regional Studies are Needed in the Development of Full-scale Integrated Assessment Modelling of Global Change Processes. Global Environmental Change **7,** 337-356.

Environment Canada, 1999. Canadian Prairie Daily Climate Data CDRom.

Environmental Systems Research Institute, Inc. (ESRI), 380 New York Street, Redlands, CA 2001.

Flato, G.M. and Hibler, W.D. III, 1992. Modelling Pack Ice as a Cavitating Fluid. Jounral of Physical Oceanography **22,** 626-651.

Flato, G.M., Boer, G.J., Lee, W.G., McFarlane, J.A., Ramsden, D., Reader, M.C., Weaver, A.J. 2000. The Canadian Centre for Climate Modelling and Analysis Global Coupled Model and its Climate. Climate Dynamics **16,** 451-467.

Frakes, B. and B. Yarnal, 1997. A procedure for blending manual and correlation-based synoptic classifications. International Journal of Climatology **17,** 1381-1396.

Fyfe, J.C., and G.M. Flato, 1999. Enhanced climate change and its detection over the Rocky Mountains. Journal of Climate **12(1),** 230-243.

Giorgi, F. and L.O. Mearns, 1991. Approaches to the Simulation of Regional Climate. A Review. Reviews of Geophysics **29,** 191-216.

Gordon C., Cooper C., Senior C.A., Banks H.T., Gregory J.M., Johns T.C., Mitchell J.F.B. & Wood R.A. 2000. Simulation of SST, sea ice extents and ocean heat transports in a version of the Hadley Centre coupled model without flux adjustments Climate Dynamics **16,** 147-168

Grant, L. O., and A. M. Kahan. 1974. Weather modification for augmenting orographic precipitation. Weather and Climate Modification, W. N. Hess. Ed., John Wiley and Sons: 282-317.

Gregory, J. M., J. A. Church, and G. J. Boer, K. W. Dixon, G. M. Flato, D. R. Jackett, J. A. Lowe, S. P. O'Farrell, E. Roeckner, G. L. Russell, R. J. Stouffer, and M. Winton: 2001. Comparison of results from several AOGCMs for global and regional sea-level change 1900-2100. Climate Dynamics **18,** 225-240.

Grotch, S.L., and M.C. MacCracken. 1991. The use of general circulation models to predict regional climate change. Journal of Climate **4,** 286-303.

Hamilton, K. P., R. J. Wilson, and R. Hemler. 2001. Spontaneous stratospheric QBO-like oscillations Simulated by the GFDL SKYHI general circulation model. Journal of the Atmospheric Sciences **58,** 3271-3292.

Hay, L., McCabe, G.J. Jr., Wolock, D.M. and Ayers, M.A. 1991. Simulation of precipitation by weather type analysis. Water Resources Research **27,** 493-501.

Hengeveld, H.G. Projections from Canada's Climate Future - a discussion of recent simulations with the Canadian Global Climate Model. Meteorological service of Canada Environment Canada 2000

Hewitson, B.C. and R.G. Crane, 1996. Climate Downscaling: Techniques and Applications. Climate Research **7,** 85-95.

Hungerford, R.D., R.R. Nemani, S.W. Running, and J.C. Coughlan, 1989. MTCLIM: Mountain Microclimate Simulation Model. Research Paper INT-414. Ogden, UT: U.S. Department of Agriculture, Forest Service, Intermountain Research Station.

Huth, R. 1996. A intercomparison of computer-assisted circulation classification methods. International Journal of Climatology **16,** 893-922.

IPCC, 1996. Climate Change 1995. The Science of Climate Change. Contribution of the Working group I to the Second Assessment Report of the IPCC. Houghton, J.T., L.G. Meira Filho, B.A. Callander, N. Harris, A. Kattenburg and K. Maskell (eds.). Cambridge University Press, Cambridge, UK, 572.

IPCC. 1996a. Climate Change 1995. The Science of Climate Change. Contribution of Working Groups I to the Second Assessment Report of the Intergovernmental Panel on Climate Change. Cambridge University press, NY.

IPCC. 1996b. Climate Change 1995. Impacts, Adaptations and Mitigation of Climate Change: Scientific-Technical Analyses. Contribution of Working Group II to the

Second Assessment Report of the Intergovernmental Panel of Climate Change. Cambridge University Press, NY.

Johnson, G.L., and C.L. Hanson. 1995. Topographic and atmospheric influences on precipitation variability over a mountainous watershed, Journal of Applied Meteorolology **34,** 68-87.

Jones P.D., Horton E.B., Folland C.K., Hulme M., Parker D.E. & Basnett T.A. 1999 The use of indices to identify changes in climatic extremes. Climatic Change **42,** 131-149

Jones, P.D. 1994. Hemispheric Surface Air Temperature Variations: A Reanalysis and an Update to 1993. Journal of Climate **7,** 1794-1802.

K. Runions, Alberta Environment, personal communication, 2001

Keeling, C.D. and T.P. Whorf. 2001. Atmospheric CO_2 records from sites in the SIO air sampling network. In Trends: A Compendium of Data on Global Change. Carbon Dioxide Information Analysis Center, Oak Ridge National Laboratory, U.S. Department of Energy, Oak Ridge, Tenn., U.S.A. http://cdiac.esd.ornl.gov/trends/co2/sio-mlo.htm

Key, J. and Crane, R.G. 1986. A comparison of synoptic classification schemes based on "objective" procedures. Journal of Climatology **6,** 375-388.

Kidson, J.W. and Thompson, C.S. 1998. Comparison of statistical and model-based downscaling techniques for estimating local climate variations. Journal of Climate **11,** 735-753.

Kind, R.J., 1981, 'Snowdrifting' in D.M. Gray and D.H. Male (eds.), Handbook of Snow-Principles, Processes, Management & Use, Pergamon Press, Toronto, pp. 338-359.

Kirchhofer, W. 1973. Classificationof European 500mb patters, Arbeitsbericht der Schweizerischen Meteorologischn Zentralanstalt **43.** Geneva.

Klein, W.H. and J.M. Klein, 1984. The synoptic climatology of monthly mean surface temperature in the United States during winter relative to the surrounding 700-mb height field. Monthly Weather Review **112,** 433-448.

Klein, W.H. and J.M. Klein, 1986. The synoptic climatology of monthly mean surface temperature in the United States during summer relative to the surrounding 700-mb heigh field. Monthly Weather Review **114,** 1231-1250.

Kondrad, C.E. II.1997. Synoptic-scale features associated with warm season heavy rainfall over the interior southeastern United States. Weather and Forecasting **12,** 557-571.

Krichak, S.O., Tsidulko, M., Alpert, P. 2000. Monthly synoptic patterns associated with wet/dry conditions in the eastern Mediterranean. Theoretical Applied Climatology **65,** 215-229.

L. Flanagan, University of Lethbridge, personal communication, 2001.

Lamb, H.H. 1972. British Isles Weather Types and a Register of the Daily Sequence of Circulation Patterns. 1861-1971

Lapp, S., Byrne, J., Kienzle, S. and I. Townshend. 2001. Linking GCM synoptics and precipitation for western North America. International Journal of Climatology Under Review.

Latif, M. and T.P. Barnett. 1996. Decadal Climate Variability over the North Pacific and North America: Dynamics and Predictability. Journal of Climate **9,** 2407-2423.

Leith, R.M. and P. Whitfield. 1998. Evidence of Climate Change Effects on the Hydrology of Streams in South-Central B.C. Canadian Water Resources Journal **23,** 219-230.

Leydecker, A. and J. M. Melack. 1999. Evaporation from Snow in the Central Sierra Nevada of California. Nordic Hydrology **30,** 81-108.

Lund, I.A. 1963. Map-pattern cliassification by statistical methods. Journal of Applied Meteorology **2,** 56-65.

Marks, M., Domingo, J., Susong, D., Link, T., and D. Garen. 1999. A spatially distributed energy balance for application in mountain basins, Hydrological Processes. **13,** 1935-1959.

McCabe, G.J. 1995. Jr., Relationships between atmospheric circulation and height anomalies and 1 April Snowpack accumulations in the western USA, International Journal of climatology **15,** 517-530,.

McFarlane, N.A., G.J. Boer, G.J., J.P. Blanchet, and M.J. Lazare. 1992. The Canadian Climate Centre Second-Generation General Circulation Model and Its Equilibrium Climate, Journal of Climate **5,** 1013-1044.

Muller, R.A., and C.L. Wax, 1977. A comparative synoptic climatic baseline for coastal Louisiana, Geosci. Man. **18,** 121-129.

Murphy, J.M. 1999. An evaluation of statistical and dynamical techniques for downscaling local climate. Journal of Climate **12,** 2256-2284.

Murphy, J.M. 2000. Predictions of climate change over Europe using statistical and dynamical downscaling techniques. International Journal of climatology **20(5),** 489-501.

National Climate Data Center, 2000. http://lwf.ncdc.noaa.gov/oa/ncdc.html

Osborn, T.J. and Hulme, M. 1997. Development of a relationship between station and grid-box rain-day frequencies for climate model evaluation. Journal of Climate **10,** 1885-1908

Osborn,T.J., Conway, D., Hulme, M., Gregory, J.M. and Jones, P.D. 1999. Air flow influences on local climate: observed and simulated mean relationships for the UK. Climate Research **13,** 173-191.

Pearman, G.I. Global climate change and the energy community. Limiting greenhouse effects: controlling carbon dioxide emissions. Report, Dahlem workshop, Berlin, 1990. (Wiley; Environmental Sciences Research Report, ES 10), 1992, pp 1-12.

Pipes, A. and M.C. Quick, 1977. UBC Watershed Model Users Guide. Department of Civil Engineering, University of British Columbia.

Pomeroy, J.W. and Gray, D.M. 1994, Sensitivity of snow relocation and sublimation to climate and surface vegetation', in H.G. Jones, T.D. Davies, A. Ohmura, and E.M. morris (eds.), Snow and Ice Covers: Interactions with the Atmosphere and Ecosystems, IAHS Publ. No. 223, Wallingford, pp. 213-225.

Pomeroy, J.W. and Male, D.H. 1998. Optical properties of blowing snow, Journal of Glaciology **34,** 3-9.

Rama, S., Reddy, C. and C. Price. 1999. Carbon sequestration and conservation of tropical forests under uncertainty. Journal of Agricultural Economics **50**, 17-35.

Reader, C. and G.J. Boer. 1997. The modification of greenhouse gas warming by the direct effect of sulphate aerosols. Climate Dynamics **14,** 593-608.

Reader, M.C., and Boer, G.J., 1998. The modification of greenhouse gas warming by the direct effect of sulphate aerosols. Climate Dynamics **14,** 593-607.

Rind, D., P. Demenocal, G.L. Russell, S. Sheth, D. Collins, G.A. Schmidt, and J. Teller 2001. Effects of glacial meltwater in the GISS Coupled Atmosphere-Ocean Model: Part I: North Atlantic Deep Water response. Journal of Geophysical Research **106,** 27335-27354.

Rinke, A., Lynch, A.H. and K. Dethloff. 2000. Intercomparison of Arctic regional climate simulations: Case studies of January and June 1990. Journal of Geophysical Research D: Atmospheres **105**, 29669-29683.

Saunders, I.R. and J.M. Byrne. 1994. Annual and seasonal climate and climatic changes in the Canadian prairies simulated by the CCC GCM. Atmosphere Ocean **32,** 621-641.

Saunders, I.R. and J.M. Byrne. 1996. Generating regional precipitation from observed and GCM synoptic-scale pressure fields, Southern Alberta, Canada. Climate Research **6,** 237-249.

Schlesinger, M.E., and J.F.B. Mitchell. 1987. Climate model simulations of the equilibrium climatic response to increased carbon dioxide. Rev. Geophys. **25,** 760-798.

Schmidt, R.A. 1982. Properties of blowing Snow, Rev. Geophysical. Space Physics **20,** 39-44.

Schmidt, R.A.1972. Sublimation of wind-transported snow-A Model. Res. Pap. RM-90, Rocky Mt. For and Range Expr. St., For. Serv., U.S. Dept. of Agric., Fort Collins, Colo.

Sheppard, Dennis L., 1996. Modelling hydrometeorology in the Upper Oldman River basin. Master of Science thesis, University of Lethbridge, Canada, 178 pp.

Shindell, D.T., G.A. Schmidt, M.E. Mann, D. Rind, and A. Waple. 2001. Solar forcing of regional climate change during the Maunder Minimum. Science **294,** 2149-2152.

Singh, V. 1992. Elementary Hydrology. Prentice Hall, Englewood Cliffs, NJ. Pp 349.

Thorpe, A.D. and Mason, B.J. 1966. The evaporation of ice spheres and ice crystals. British Journal of Applied Physics **17,** 541-548.

Trenberth, K.E. 1990. Recent Observed Interdecadal Climate Changes in the Northern Hemisphere. Bulletin of the American Meteorological Society **71**, 988-993.

Trigo, R.M. and C.C. DaCamara. 2000. Circulation weather types and their influence on the precipitation regime in Portugal. International Journal of climatology **20(13),** 1559-1581.

Valdes, P.J. 2000. South American palaeoclimate model simulations: How reliable are the models? Journal of Quaternary-Science **15**, 357-368.

Venugopal, V. Foufoula, G.E., and V. Sapozhinikov. 1999. A space-time downscaling model for rainfall. Journal of Geophysical Research D: Atmospheres. Aug 27 **104,** 705-19, 721.

Venzke S., Allen, M.R., Sutton R.T. & Rowell D.P., 1999. The atmospheric response over the North Atlantic to decadal changes in sea surface temperature. Journal of Climate **12,** 2562-2584.

Verseghy, D.L., N.A. McFarlane, and M. Lazare, 1993: A Canadian Land Surface Scheme for GCMs:II. Vegetation model and coupled runs. International Journal of climatology 13, 347-370.

von Storch, H. 1995. Inconsistencies at the interface of climate impact studies and global climate research. Meteorol. Zeitschrift **4** , 72-80.

von Storch, H. 1999. The global and regional climate system. In Anthropogenic Climate Change. Ed. by H. von Storch and G. Flöser. Springer Verlag, ISBN 3-540-65033-4, pp. 3B36.

von Storch, H., E. Zorita, and U. Cubasch. 1993. Downscaling of global climate change estimates to regional scales: An application to Iberian winter rainfall. Journal of Climate **6,** 1161-1171.

von Storch., H. .1999. Representation of conditional random distributions as a problem of "spatial" interpolation. In. geoENV II - Geostatistics for Environmental Applications. Ed. by J. Gòmez-Hernàndez, A. Soares and R. Froidevaux. Kluwer Adacemic Publishers, Dordrecht, Boston, London, ISBN 0-7923-5783-3, pp. 13B23.

Widmann, M., C. S. Bretherton, and E. P. Salathé Jr. 2002. Statistical precipitation downscaling over the Northwestern United States using numerically simulated precipitation as a predictor. Journal of Climatology submitted.

Wilby, R. 1995. Simulation of precipitation by weather pattern and frontal analysis. Journal of Hydrology **173,** 91-109.

Wilby, R. Greenfield, B. and C. Glenny. 1994. A coupled synoptic-hydrological model for climate change impact. Journal of Hydrology **153,** 265-290.

Williams, J.R. 1999. Addressing global warming and biodiversity through **forest** restoration and coastal wetlands creation. Science of the Total Environment **240,** 1-9.

Woodhouse, C.A. 1997. Winter Climate and Atmospheric Circulation Patterns in the Sonoran Desert Region, USA. International Journal of climatology **17,** 859-873.

Wyman, R.R. 1995. Modeling snowpack accumulation and depletion. IN: Guy, B.T. and J. Barnard (editors). Mountain Hydrology Peaks and Valleys in Research and Applications Conference Proceedings, May 16-19, 1995. Canadian Water Resources Association, Cambridge.

Xiuqing, Z., Van Liew, M.W. and G.N. Flerchinger. 2001. Experimental study of infiltration into a bean stubble field during seasonal freeze-thaw period. Soil Science **166,** 3-10.

Yarnal, B, 1984. Synoptic-scale atmospheric circulation over British Columbia in relation to the mass balance of Sentinel Glacier. Annual Association of American Geographers 74, 375-392.

Yarnal, B. and B. Franks. 1996. Using synoptic climatology to define representative discharge events. International Journal of Climatology, **17,** 323-341.

Yarnal, B. and H.F. Diaz. 1986. Relationships between extremes of the southern oscillation and the winter climate of the anglo-american Pacific Coast. Journal of Climatology **6,** 197-219.

Yarnal, B. and White, D.A. 1987. Subjectivity in a computer-assisted synoptic climatology I: classification results. Journal of Climatology **7,** 119-128.

Yarnal, B., White, D.A. and Leathers D.J. 1988. Subjectivity in a computer-assisted synoptic climatology II: Relationships to surface climate. Journal of Climatology **8,** 227-239.

Zhang, G.J. and N. A. McFarlane. 1995. Sensitivity of climate simulations to the parameterization of cumulus convection in the CCC-GCM. Atmosphere Ocean **3,** 407-446.